



LIQUID CRYSTALLINE EPOXY BASED THERMOSETTING POLYMERS¹

C. CARFAGNA^{a,*}, E. AMENDOLA^b and M. GIAMBERINI^a

^aUniversity of Naples ‘‘Federico II’’, Department of Materials and Production
Engineering, Piazzale Tecchio 80, 80125 Naples, Italy

^bInstitute for Composite Materials Technology, National Research Council, Piazzale
Tecchio 80, 80125 Naples, Italy

Abstract – In recent years many examples of liquid crystalline thermosetting polymers have been reported in the literature. The main reason for the development of this new class of materials comes from both technological and theoretical implications. Among the different anisotropic thermosets, epoxy resins represent a family of polymers whose properties make them primary candidates in different fields ranging from high performance matrices in advanced composites to polymers for optical applications. The chemistry of curing process of amine hardened conventional epoxy resins is well known from the literature; however some substantial differences arise during liquid crystalline epoxy monomers crosslinking. The level of order of the cured resin can be strongly affected by the nature of the hardener, as well as the physical properties of the cured material. This review will present the results of synthesis and physico-chemical characterization of liquid crystalline epoxy resins in relation to their applications in some specific fields. © 1997 Elsevier Science Ltd.

*Principio caeli clarum purumque colorem,
quaeque in se cohibet, palantia sidera passim,
lunamque et solis praeclara luce nitorem;
omnia quae nunc si primum mortalibus essent,
ex improvise si sint obiecta repente,
quid magis his rebus poterat mirabile dici
aut minus ante quod auferent fore credere gentes?*

*Glaze the pure and clean colour of the sky
and what it contains in itself, stars wandering here and there
and the moon, and the sunshine, of magnificent light
All things that should they now appear to the mortals for the first time
Should they suddenly stare at us,
What could we tell more wonderful
Or what else would the peoples dare to expect?
(Tito Lucrezio Caro, De Rerum Natura, Liber Secundus, 1030–1035)*

¹This paper is dedicated to R. S. Bauer.

CONTENTS

Introduction	1608
Physical properties of amine cured liquid crystalline epoxy resins (LCER)	1611
Curing kinetics of LCER with aromatic amines	1620
Lightly crosslinked LCER	1626
Orientation of LCER	1637
LCER as matrix for polymer dispersed liquid crystals (PDLC)	1641
References	1645

1. INTRODUCTION

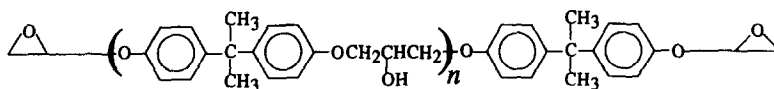
Epoxy Resins are thermosetting polymers known from many decades. The wide diffusion they have found on the market is a consequence of their extreme versatility. In fact their applications range from laminated circuit board, carbon fiber composites, electronic component encapsulations and adhesives.¹ At the present almost 90% of the world production of Epoxy Resins is based on the reaction between Bisphenol A (2,2-bis(4'-hydroxyphenyl)propane and epichlorohydrin.²⁻⁴ The resulting glycidyl terminated monomers can contain one or more Bisphenol A groups, depending on the required applications [Fig. 1(a)].⁵ Curing can result in a tridimensional network with properties depending on the extent and density of crosslinking. Aromatic amines generally lead to thermosets with higher Tgs, superior thermal resistance and mechanical performances. If aliphatic acids are used as curing agents a more flexible material will result with lower Tg.⁶

The increasing demand of new materials for aircraft industry has pushed resin suppliers to work on new systems to meet the requirements for high performance composite applications. Their attention was previously directed towards resins containing more glycidyl groups per molecule, keeping however unchanged the kinked geometry of monomeric skeleton [Fig. 1(b)]. Increased crosslinking extent, although results in a higher Tg, always leads to systems characterized by lower toughness. Therefore chemists concentrated also towards the incorporating of big groups, such as fluorene, in thermosetting resins [Fig. 1(c)] in order to improve their fracture resistance.

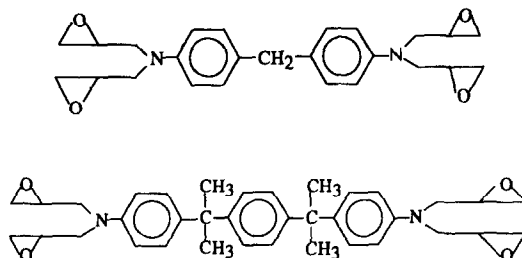
Nowadays high Tg materials have been produced without solving the drawback that is considered the *Achille's heel* of this class of materials, i.e. their brittleness. Many efforts were directed towards the increase of toughness by means of including functionalized rubbers in glassy thermosets.⁷ However higher fracture energies are negatively balanced by a Tg reduction and a consequent decrease of the mechanical properties.

Therefore, for what composite applications are concerned, the goal is to design resins with high Tg, high modulus and superior fracture toughness. In the last 25 years, together with the demand of new high performance polymers, the scientific community devoted much efforts to the synthesis of liquid crystalline polymers.⁸⁻¹⁰

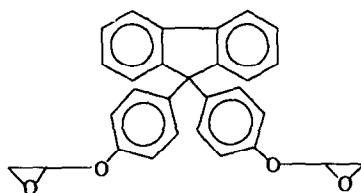
Universities and Industries engaged resources in the development of new polymers with outstanding properties: main-chain fully aromatic polymers, flexible spaced, side-chain, comb-like polymers... scientific literature is full of this terminology. In the beginning it seemed that LCPs (this is the term that collects all the family of *liquid crystalline polymers*) should replace classical polymers for high performance applications, and polymer scientists



a



b



c

Fig. 1. Epoxy resins containing Bisphenol A (a), more glycidyl groups per molecule (b), fluorene groups (c).

who were not involved in this research ran the risk to be considered out of the time... However, it was quickly realized that LCPs could not find wide diffusion on the market due to the costs of the raw materials in general, and to the synthesis that is often very expensive. To tell the truth, LCPs were very unlucky because they were developed in a period in which a worldwide market crisis reduced research resources devoted to the production of new high performance polymers. In any case LCPs probably paid the cost due to the fact that their applications were addressed in market segments where *classical polymers* are well rooted, instead of opening new windows based on their peculiarity. However, a full treatment on the market politics of polymer industry is beyond the aim of this paper. In 1990

the world consumption of thermotropic LCPs ranged around 5 million pounds, a large part of which comprised injection molded parts.¹¹ Although the outstanding mechanical performances of the oriented LCPs, along the draw direction, a severe weakness in the orthogonal direction represents a dramatic limitation in their applicability.^{12,13} This is the most criticized parameter, which, coupled to the above economical considerations, clipped LCPs wings for their wide market diffusion, according to our opinion. The above mentioned problem related to the improvements of the interchain bonding justified the initial work of industrial researchers on the possibilities of crosslinking linear LCPs.

Surprisingly the first theoretical work on LCPs were directed by de Gennes on the analysis of the properties of liquid crystalline monomers after crosslinking. An early communication of 1975 begins with: "*Nous avons discuté autrefois certains aspects théoriques de la reticulation en phase mésomorphe...*"¹⁴ At the beginning, in 1975, de Gennes suggested that nematic polymers might be crosslinked to produce networks of quite remarkable properties, for instance non-linear or discontinuous stress-strain relations. The basic idea was that an isotropic phase responds to a weak applied external field by developing weak small nematic order. As the field is increased, a discontinuous jump to a high state of nematic order occurs, provided that the temperature is not above some critical value (T_c) (Fig. 2). Above this critical value the transition is washed out, however large the field is. In order that the theory can be supported by experiment, the crosslinking process should lead to a well-determined number of crosslinks of known functionality. Networks should not be too highly crosslinked if a correlation with a Gaussian (classical) theory of rubber is to be sought.

Since the initial work of de Gennes an increasing interest was shown by the scientific community on the liquid crystalline thermosets (LCT), as can be summarized in Table 1. The industrial interest on liquid crystalline epoxy resins (LCER) is very recent, in fact only in the late 1980s main chemical industries patented their results on LCER.¹⁵⁻¹⁷ If geometry of Bisphenol A is taken into account, it can be easily shown that this molecule is kinked: therefore, in order to get a liquid crystalline structure for cured epoxy resin, new glycidyl terminated monomers, having a rigid skeleton, needed to be synthesized. In Fig. 3 the rigid monomers, of interest to the scientific community for the production of LCER, are shown.

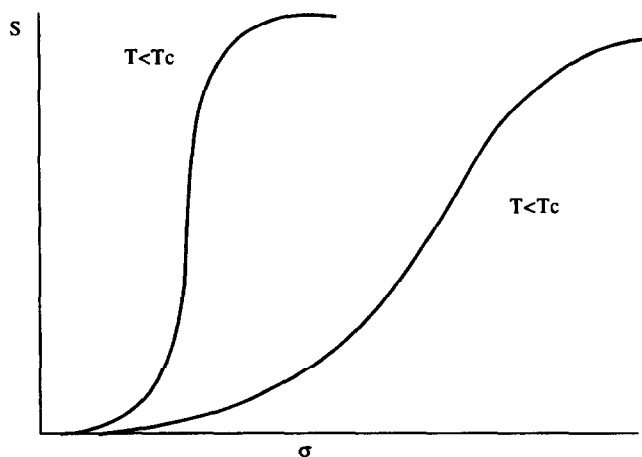


Fig. 2. Order parameter vs applied stress according to the de Gennes theory.

Table 1. Milestones of liquid crystalline thermosets

Herz	<i>J. Polym. Sci. C</i> , 1275 , 1963	Curing of sodium styrylundecanoate-water with divinylbenzene
Blumstein	<i>J. Colloid Interface Sci.</i> , 31 (2), 236, 1969	Curing of quasi-smectic layers of polar molecules
P.G. de Gennes	<i>Phys. Lett</i> , A28 , 1969	Theoretical approach
Strzelecki	<i>Bull. Soc. Chem (France)</i> , 597 , 1973	Crosslinked diacrylate Schiff base
Finkelmann	<i>Makromol. Chem. Rapid Comm.</i> , 2 , 317, 1981	LC elastomers
Hikmet	<i>Makromol. Chem.</i> , 190 , 3201, 1989	Photopolymerization of diacrylates
Bayer	Patent activity	LC epoxy resins
Dow	1988	
Ober	1990	LC epoxy resins
Rozenberg		
Carfagna		
Mikroyannidis		
Broer		
Zentel		
Szczepaniak		

In this review the chemistry and the physical properties of epoxy based liquid crystalline thermosets will be examined.

2. PHYSICAL PROPERTIES OF AMINE CURED LIQUID CRYSTALLINE EPOXY RESINS (LCER)

Physical properties of conventional epoxy resins are strongly affected by curing reactions. Curing extent and density have a dramatic consequence on the properties of the thermoset. As far as the mechanical properties are concerned, tensile strength has always been found lower than those expected on the basis of weak Van der Waals interactions. This has been ascribed to the presence of defects in the matrix during the cure.^{18,19} These defects, whose origin is absolutely statistical, play a fundamental role on the fracture resistance.

It has been found²⁰ that the fracture energies of linear glassy polymers are much higher than those exhibited by brittle epoxy resins. This is accounted in the theories of fracture by the ability of the matrix to undergo plastic deformation (Fig. 4).^{21,22}

Crack propagation in a brittle thermoset involves localized viscoelastic and plastic energy absorbing processes at the crack tip. Plastic deformation can be achieved either by crazing or shear yielding. The difference consists in the fact that crazing involves cavitation, resulting in a volume increase, while shear yielding occurs at constant volume. For cured epoxy resins crazing is possible without significant bond breaking. The formation of short microcraze structures involving nodules with dimensions of 5–10 nm has been supposed by several authors for classical epoxies.^{23–25} They suggested that crazing can be reduced by the presence of nodules. However, this mechanism of deformation is possible only if the internodular region is constituted by weakly crosslinked and easily deformable portions. Therefore, it is assumed that the localized inhomogeneities between regions with different crosslink density can reduce the brittleness of epoxy resins. The resulting toughness can be improved if the

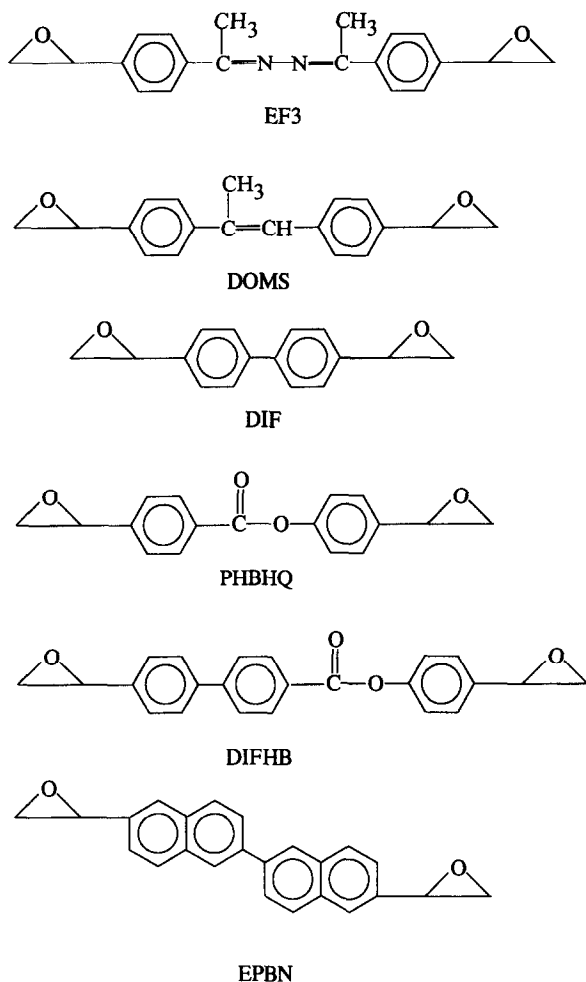


Fig. 3. Rigid monomer skeletons for the production of LCER.

crack proceeds around more highly crosslinked regions connected by the weaker internodular matrix.

Physical properties of LCER depend on the state of order of the cured thermoset.²⁶ For mesomorphic polymers in general, the order parameter represents the statistical distribution of the orientation of the different mesogenic units:

$$S = \frac{1}{2} \langle 3 \cos^2 \Theta - 1 \rangle$$

where Θ is the angle between the rigid-rod molecule and a preferred direction, defined by the director \mathbf{n} , which gives the average molecular alignment direction in the anisotropic sample.

The bulk polymer is constituted by many domains, within which the orientation of the rigid molecular portions have an orientational correlation. If no electric, magnetic or mechanical field previously oriented the polymer, the different domains result randomly oriented and the

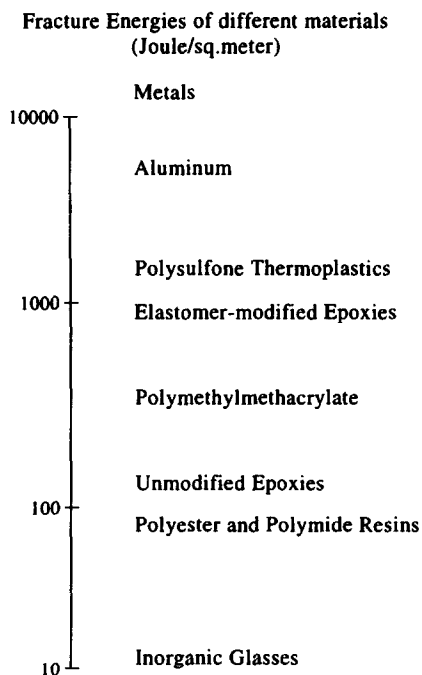


Fig. 4. Fracture energies (Joule/m²) of different materials.

order parameter is low. In the case of crosslinked polymers, alike for thermotropic ones, the cured resin can exhibit a multidomain morphology that can be shown by means of optical microscopy.

A correlation between fracture toughness and the curing temperature of the epoxy resin is shown in Fig. 5. By increasing curing temperature from 120° to 170°C, toughness is reduced to about 50%. The lower fracture toughness at higher temperatures is due to the progressive reduction of the extent of nematic portions and the progressive increase of the isotropic parts of the cured resin, as revealed by optical microscopy. The density of the cured resin progressively decreases with increasing curing temperature, indicating that at higher temperatures the extent of ordered domains, acting as nodules around which cracks can deviate, decreases (Fig. 6).

In other terms, the microstructure of LCER, having overall isotropic properties, consists of anisotropic domains with properties, such as strength, different along and across their molecular orientations. This results in the deviation of crack propagation from a straight line and suggests that inhomogeneities and localized anisotropy of the nematic structure are the main reasons for the fracture toughness increase in the liquid crystalline material.

In order to emphasize the differences in the physical properties attributed to morphology and phase structure, the same epoxy-amine mixture has been cured both in the liquid crystalline and isotropic state by simply varying the proper curing temperature. A comparison among the physical properties exhibited by the epoxy resins cured in the liquid crystalline or in the isotropic state respectively, is reported in Table 2.

The most significant differences lie in the fracture toughness, density and coefficient of

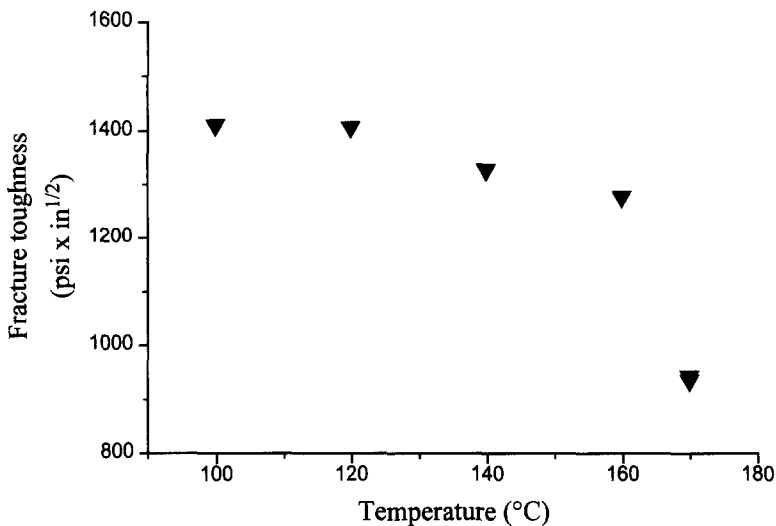


Fig. 5. Fracture toughness vs curing temperature for a liquid crystalline epoxy resin.

thermal expansion (CTE). For what density and toughness are concerned, an explanation has been already given above. Regarding CTE, the lower values found for the resin cured in the liquid crystalline state are in line with the results found for thermotropic polymers, for which CTE values are always lower than in the case of amorphous polymers. The resin cured in the liquid crystalline state has a T_g 5 degrees higher than the isotropic one. Normally for anisotropic networks lower T_g s have been reported with respect to those of the isotropic ones. In the case of polyacrylate,²⁷ the differences were not ascribed to a different crosslink density, but to the physical crosslinks present in the isotropic network. They act as extra

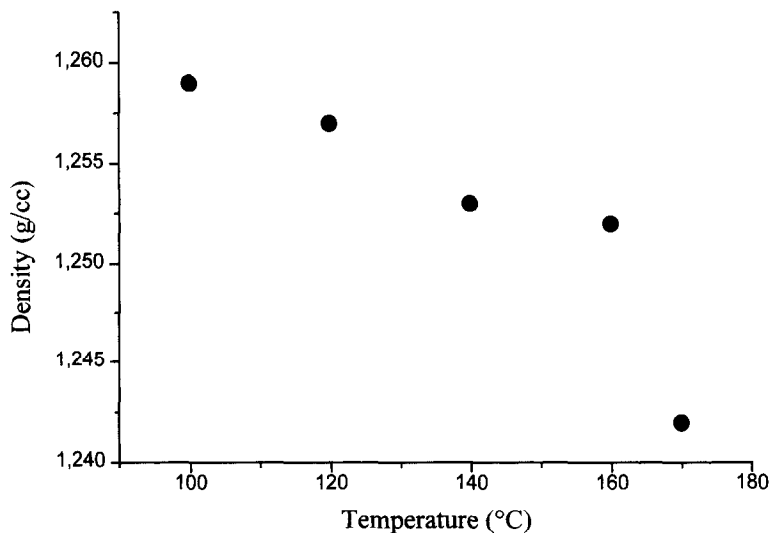


Fig. 6. Density vs curing temperature for a liquid crystalline epoxy resin.

Table 2. Physical properties of an epoxy-amine system cured in the liquid crystalline and isotropic phase

Structure	Strength (Ksi)	Strain %	Modulus (Ksi)	Tg (°C)	CTE (10 ⁻⁶ /°C)	Kq (psi* in ^{1/2})
LC	15.8	8.0	334	230	50	1200
ISO	16.2	8.3	328	225	60	780

constrains, thus contributing to increasing the Tg of the isotropic material. In analogy with the systems described in literature, we can suppose that also in the case of epoxy resins a larger presence of physical crosslinks should enhance the Tg of the isotropic resin. However, as above reported,²⁸ curing in the liquid crystalline state involves better reactivity of the functional groups, enhancing the extent of the chemical crosslinks which are clearly much more effective in increasing the Tg of the network than the physical ones.

Flexural properties are not affected by the state of order of the cured thermoset. The small differences are not significant to justify any comment. Probably one would have expected higher modulus in the case of the resin cured in the nematic phase. Nevertheless, the overall properties of the thermoset, although it has been hardened in a liquid crystalline state, are isotropic in absence of any orientation of the director: as a consequence, no increase in modulus values can be expected.

The water sorption isotherms in epoxy resins have been described in terms of multimodal sorption, including molecular dissolution in the equilibrium polymer matrix, adsorption on the surface of non-equilibrium microcavities (excess free volume "frozen" in the glassy polymer matrix), and adsorption on specific hydrophilic sites, such as unreacted amines.²⁹ The first two modes are typically observed when low molecular weight penetrants adsorb in glassy polymers, while the third mode is due to the chemical nature of the polymer.

Gas permeability depends on both gas solubility and diffusivity. In fact, permeability (P) can be defined as $P = S \cdot D$, where D is an average diffusion coefficient, while S is an average solubility coefficient. As a consequence, low permeability can be attained if gas solubility or gas diffusivity or both display low values.

According to literature data, the polymers exhibiting mesophasic behavior always feature excellent barrier properties to gases (i.e. low permeability), comparable to those of the less permeable thermoplastic polymers, i.e. polyacrylonitrile (PAN). It is still not clear if the low gas permeabilities typical of LCPs are to be ascribed to low gas solubilities or to low diffusivities. Discordant results are reported. In fact, in one case the low value of permeability was attributed to a low diffusion coefficient,³⁰ while in most cases researchers ascribed the low permeability values to surprisingly low solubility coefficients.³¹⁻³⁵

In Fig. 7 the vapor sorption isotherms for the epoxy resin p-(2,3-epoxypropoxy)- α -methylstilbene/p-aminoacetophenone azine (DOMS-NA2) cured in both the liquid crystalline and the isotropic state are reported. Water is absorbed to the same extent in the isotropic sample as well as in the nematic one.³⁶

An analogous behavior is reported for the apparent sorption coefficients of the isotropic and the mesomorphic forms in poly(p-phenyleneterephthalamide) (PPT) films and fibers:³⁷ water and gases were in fact found to be sorbed at the same extent in the mesomorphic as in the isotropic state of PPT.

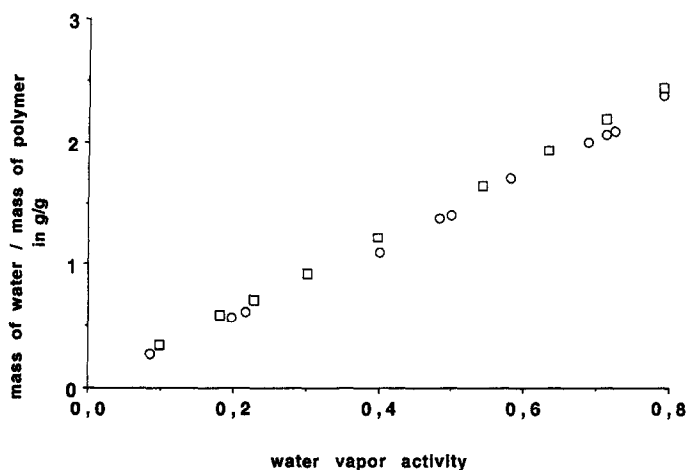


Fig. 7. Water vapor sorption isotherms at 35°C for isotropic (□) and anisotropic (O) samples (Reproduced by permission of Society of Plastics Engineers).

The shape similarity of sorption isotherms suggests that similar water sorption mechanisms are involved in the two investigated materials. Based on the isotherm shape it could be supposed that the multimodal water sorption involved in traditional epoxy resins is indeed involved in the systems under investigation.

The interpretation of water sorption measurements cannot help to gain insight into the mechanism of the hardening reaction of liquid crystalline epoxies. In fact it might be supposed that the lower viscosity of the nematic pre-gelled polymer makes the network formation easier during the diffusion controlled step of hardening. In this case, a different reactivity of the secondary amine would be observed. However, because of the reported similarities, it could be inferred that the water sorption is not affected by the state of order of the system. In other words, the nematic phase of the crosslinked resins can be achieved without modifying the chemistry of the reaction of curing. Water sorption kinetics of both anisotropic and isotropic samples were also evaluated. In Figs 8 and 9 the detected sorption kinetics are reported. The apparent water diffusion coefficients were evaluated from these data, assuming ideal Fickian behavior. The values of the diffusion coefficients do not change with the activity in both samples. The average water diffusivity is 16×10^{-9} cm²/sec for the isotropic samples and 9×10^{-9} cm²/sec for the anisotropic ones. Quite surprisingly, the rates of sorption for the two kinds of material were not very different. As reported in the literature, liquid crystalline samples generally exhibit a very low gas diffusivity and solubility. In our case neither a low water vapor solubility nor a low water vapor diffusivity was detected for the anisotropic sample. This could be partially ascribed to the specific interactions of water molecules with the polymer backbone.

The state of order of the cured thermoset is strongly affected by the nature of the curing agents. The most diffuse hardeners for epoxy resins contain amine groups. In order to evaluate the role of the curing agent and the role played by the rigid block of the epoxy monomer, we combined different compounds and examined the physical properties of the resulting thermosets (Table 3). In a previous paper²⁶ we showed that it is not so crucial that

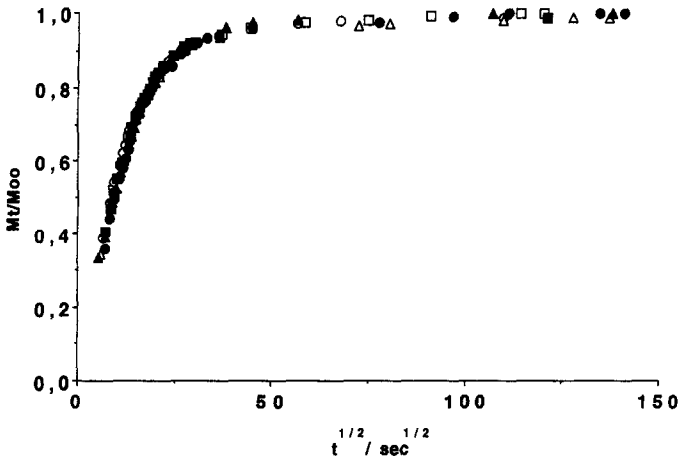


Fig. 8. Water sorption kinetics for isotropic samples at different water vapor activities. M = mass of water sorbed at time t ; M^∞ = mass of water sorbed at equilibrium. $a = 0.1$ (\square), $a = 0.302$ (\circ), $a = 0.398$ (Δ), $a = 0.542$ (\blacksquare), $a = 0.632$ (\bullet), $a = 0.789$ (\triangle). (Reproduced by permission of Society of Plastics Engineers.)

the amine curing agent has a rigid skeleton. The above reported table refers the results of the physical characterization of a glycidyl terminated monomer (DOMS), cured with a rigid aromatic diamine (NA2). By varying the curing temperature it is possible to obtain a cross-linked resin in a nematic, or isotropic structure. NA2 has a rigid structure, as it can be seen in Fig. 10(a). It was used as hardener also in the case of p-(2,3-epoxypropyl)acetophenone azine [EF3, Fig. 10(b)].

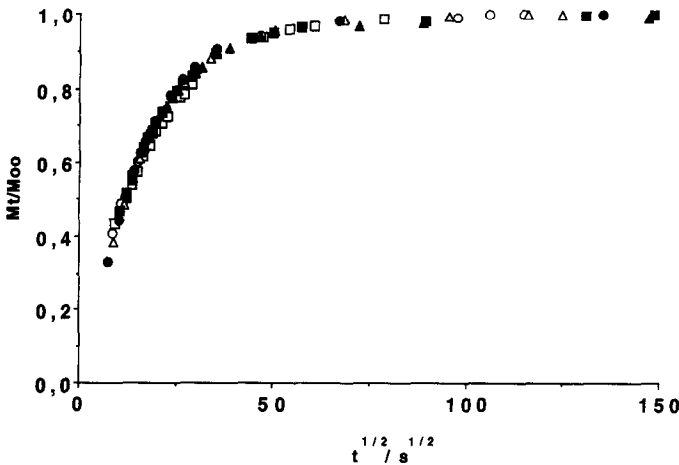
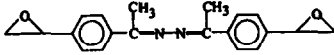
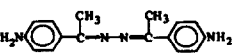
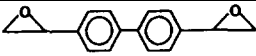
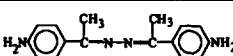
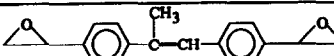

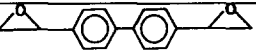

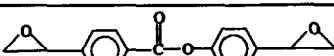
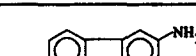
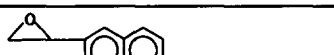


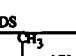
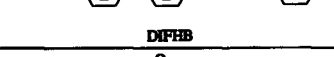
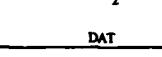
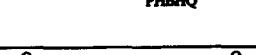
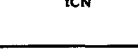


Fig. 9. Water sorption kinetics for anisotropic samples at different water vapor activities. M = mass of water sorbed at time t ; M^∞ = mass of water sorbed at equilibrium. $a = 0.085$ (\square), $a = 0.2$ (\circ), $a = 0.4$ (Δ), $a = 0.6$ (\blacksquare), $a = 0.69$ (\bullet), $a = 0.8$ (\triangle). (Reproduced by permission of Society of Plastics Engineers.)

Table 3. Glass transition temperatures of epoxy-amine systems cured at different temperatures

System		Curing temperature (°C)	T _g (°C)
Epoxy monomer - curing agent			
		170	220
		130	230
		107	138
		150	219
		120	174
		250	254
		150	178
		95	118
		180	140

The DSC dynamic analysis of the stoichiometric blend of EF3 and NA2 (Fig. 11) shows a first endothermic peak, centered at about 150°C, relative to the melting of the two components. At 170°C an exothermic peak starts, with a maximum at 195°C, ending at 240°C. At 260°C a new exotherm starts. From this analysis we can conclude that the reaction of the epoxy monomer with the curing agent starts after the melting of the two components. The curing exotherm is not complete at 240°C. By increasing the temperature, the resin is brought above the T_g , and a second peak, due to a post-cure, occurs. Curing can be performed also on larger samples put in test tubes in a thermostatic bath at 180°C. After the melting, the two components are perfectly mixed in a unique isotropic phase (transparent liquid). At this stage the reaction has not yet produced any liquid crystalline structure. On the other hand, neither the epoxy monomers or the curing agent show any liquid crystalline phase by itself. Increasing the reaction time leads to the formation of a liquid crystalline *prepolymer*, that makes itself evident by the opacity of the reaction batch. At this stage, the resin is not yet completely crosslinked, though the increased viscosity indicates that the gel point is approaching. At the end of the reaction the resin hardens and remains opaque.

The presence of reacting epoxy and amine groups prevents the intermediates from being isolated and characterized because the curing reaction is too fast in the temperature range where the phase transition should be observed. In fact, curing begins after the melting of the two components into the isotropic phase. After the reaction of the primary amine groups, a linear prepolymer forms, whose molecular weight increases with time. It is well known that the range of stability of the liquid crystalline phase for polymer is much broader than for low molecular weight compounds, and the transition temperatures increase with increasing molecular weight of the polymer.^{38,39} As long as the gel point has not been reached, it is still possible to induce isotropic-liquid crystalline phase transitions by decreasing the system temperature. Continuing the curing process in the nematic state results in the development of covalent linkages due to the reaction of secondary reactive groups which stabilize the nematic state further to the point that it cannot be destroyed by heating.

When systems are cured at temperatures higher than a certain temperature T_{ni} , which is nematic-isotropic transition temperature of the linear prepolymer, crosslinks lock the network in the isotropic state. In fact, as revealed in Fig. 12, an increase in curing temperature

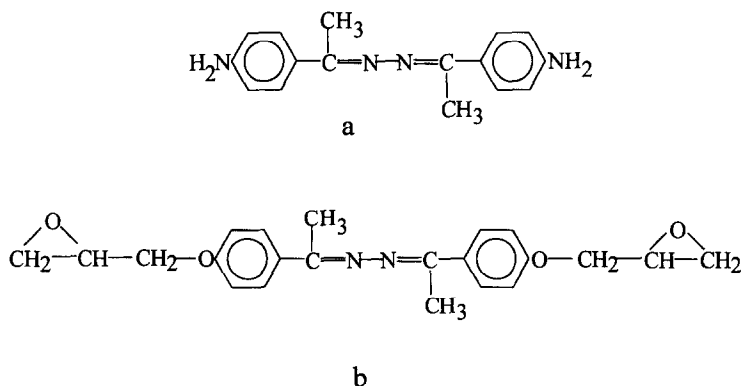


Fig. 10. Molecular formulas of NA2 (a), EF3 (b).

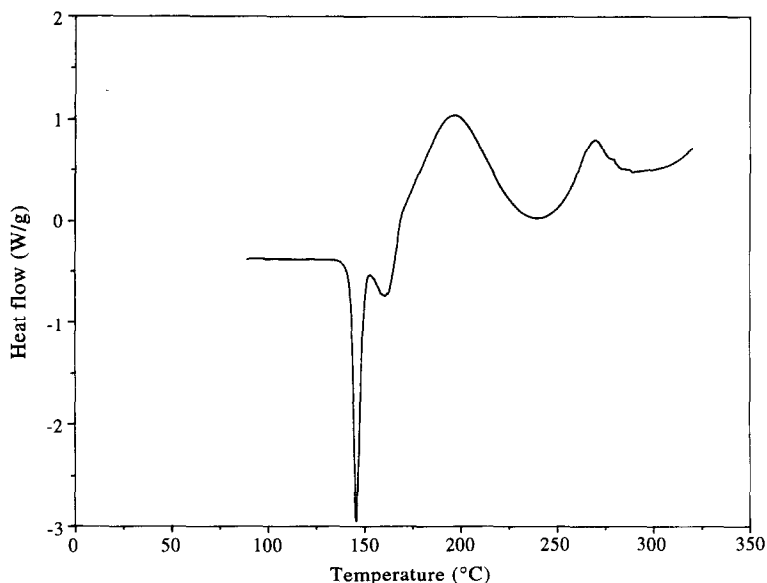


Fig. 11. DSC thermogram of a stoichiometric blend of EF3 and NA2. Heating rate 10°C/min. (Reproduced by permission of Hüthig & Wepf Verlag.)

causes a reduction of the birefringent regions leading to a two-phase material, in which the isotropic parts are progressively larger. A nematic multidomain morphology, in which the ordered parts are surrounded by disordered regions, can be supposed also for the thermoset crosslinked at lower temperatures, but in this case the isotropic regions are much less extended.

3. CURING KINETICS OF LCER WITH AROMATIC AMINES

Curing process of conventional epoxy resins with aromatic amines can be described by the mechanism reported in Fig. 13. The reaction proceeds via a nucleophilic attack of the primary amine onto the epoxy ring. The presence of water, alcohol or protons catalyzes the reaction. The hydroxyl, formed by the opening of the ring, behaves as a catalyst, determining the autocatalytic behavior of the reaction. After secondary amine is formed, a competition establishes between the addition of the primary amine, still present, and the secondary amine. It has been reported^{40,41} that the addition of the primary amine is favored with respect to the secondary, for steric hindrance reasons. In fact the kinetic constants found for the secondary amine are 2.5–5 times smaller than those found for the primary one. Nevertheless, it cannot be concluded that the addition of the secondary amine starts after the primary ones exhausted completely.^{40–45}

For the curing of LCER, a model study was reported²⁸ for the system p-(2,3-epoxypropoxy)- α -methylstilbene (DOMS) and 2,4-diaminotoluene (DAT), whose components are shown in Fig. 14. The addition of the primary amine onto the epoxy ring results in the formation of linear or slightly branched oligomers. By properly selecting the curing

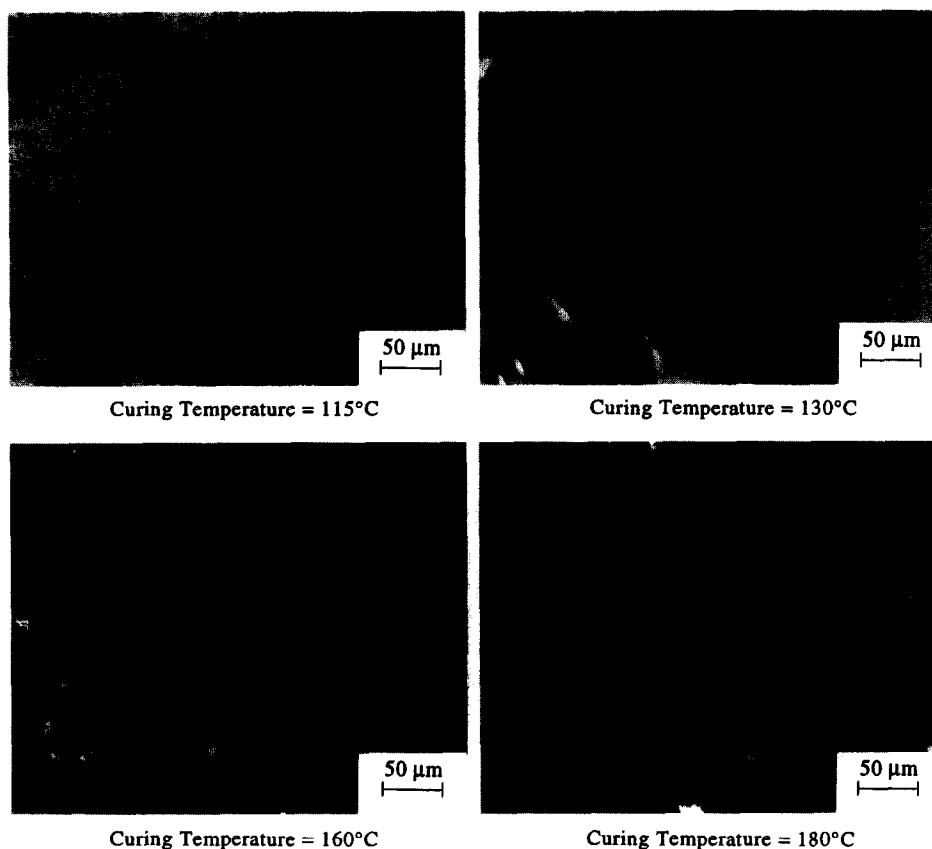


Fig. 12. Optical micrography, under crossed polarizers, of a liquid crystalline system cured at different temperatures. (Reproduced by permission of Taylor & Francis Ltd.)

temperature, the extension of the reaction determines the formation of a nematic structure, as far as a critical value of the molecular weight is reached. The formation of a tridimensional network between epoxy monomers and curing agent can be attributed to the addition of the secondary amine, as can be demonstrated by FTIR.

In the case of LCER, a mechanism not far from the above indicated can be postulated too. The curing isotherms reported at the different temperatures indicate the presence of a second maximum in the heat flow graph (Fig. 15). This second peak can be associated to a second heat release maximum due to the curing reaction of monomers in liquid crystalline phase. This hypothesis is also supported by the analysis at the optical microscope. The second maximum is washed out at 190°C. Above this temperature no birefringence could be observed at the microscope under polarized light.

The kinetic analysis of the DSC curves, in the temperature range between 150 and 170°C has led to the deconvolution of peaks and to the separate characterization of the two reactions. The method is based upon a *trial and error* procedure that can be summarized by the following steps, performed on each of the several isothermal experiments:

1. An initial tentative baseline was adopted to distinguish the contribution of the first peak

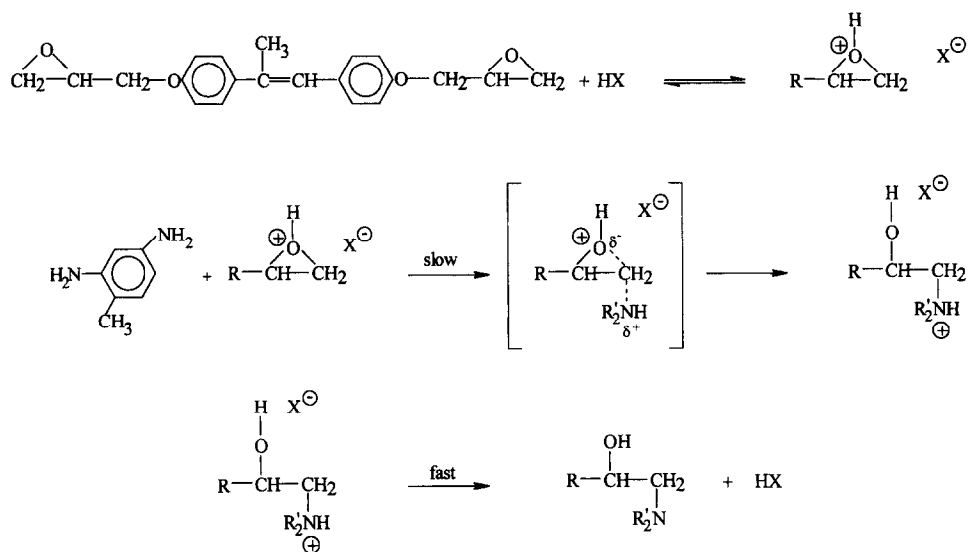


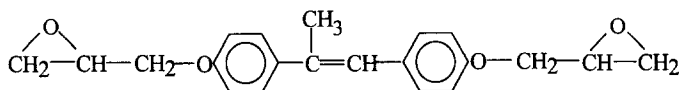
Fig. 13. Reaction mechanism of epoxy resins with aromatic amines (e.g. 2,4-diaminotoluene).

from the overall experimental data. The area under this first approximation curve was integrated to evaluate the heat of reaction associated to the first peak.

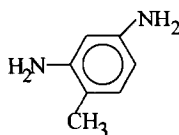
- The data table containing α vs $d\alpha/dt$ are prepared. The data relative to each temperature are simultaneously fitted applying non-linear regression, using as fitting parameters m , n , k_0 and E_a as described in the following equations:

$$\frac{d\alpha}{dt} = k \cdot \alpha^m \cdot (1 - \alpha)^n$$

$$k = k_0 \exp\left(\frac{-E_a}{RT}\right)$$



DOMS



DAT

Fig. 14. Molecular formulas of DOMS and DAT.

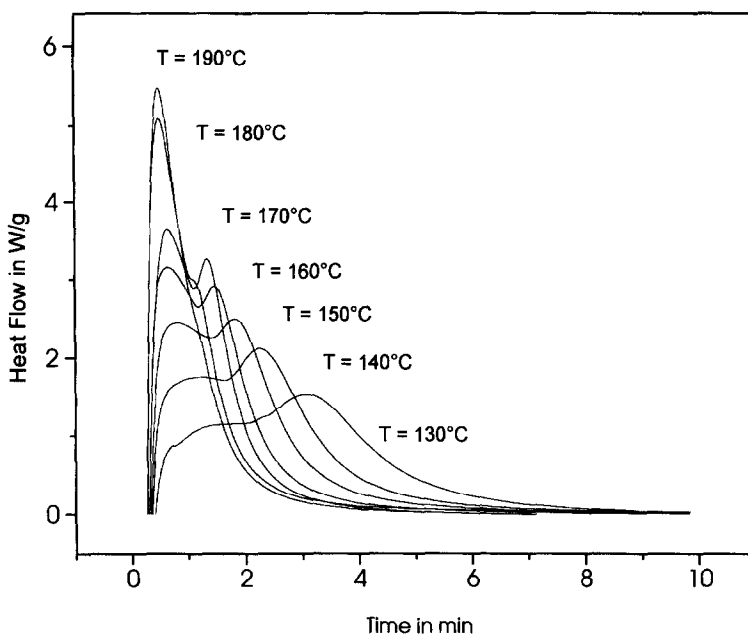


Fig. 15. DSC spectra of DOMS-DAT mixture recorded in isothermal mode at 130, 140, 150, 160, 170, 180, 190°C. (Reproduced by permission of Hüthig & Wepf Verlag.)

where k is the kinetic constant, m and n are the empirical kinetic order of reaction, k_0 is the pre-exponential frequency factor, E_a is the overall activation energy, R is the gas constant, T is the absolute temperature. The suitable range for regression has been carefully selected in order to exclude the time range where the influence of the second peak cannot be ignored.

3. The curves calculated at each temperature are compared with the experimental ones. The heat associated with the calculated theoretical curves was evaluated by scaling the computed curves until the maxima so far produced match the experimental values. This procedure is correct under the assumption that the contribution of the second exotherm to the heat flow is negligible in correspondence of the first peak.
4. The value of heat of reaction computed at the end of the first iteration is then used for the generation of a new data table containing α vs da/dt , then the procedure is again reiterated from step 2. The curves computed at the different temperatures are then subtracted from the experimental ones to isolate the contribution of the second peaks. These data are then used for a new non-linear regression to evaluate the kinetic parameters of the second peaks. The curves calculated so far are compared with the experimental data. A good matching between the traces is obtained, indicating the validity of the kinetic model adopted (Fig. 16). The results are summarized in the Tables 4–6. The activation energy associated with the first exothermic reaction is 35 kJ/mol, in agreement with typical results obtained for conventional commercial epoxy resins with polyfunctional amines. Despite the overall reaction order being 1.3, a termolecular mechanism is to be preferred.

Comparison with the results calculated for the second peak leads to some conclusions.

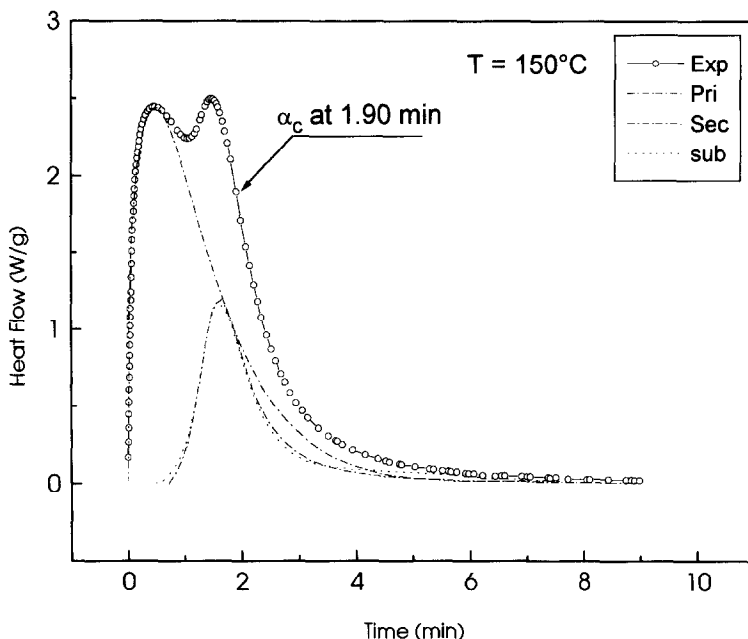


Fig. 16. DSC spectra of DOMS-DAT mixture recorded at 150°C (open circles) and comparison with calculated curves for primary and secondary amines (solid lines). The difference between experimental curve (open circles) and calculated curve for primary amine (solid line) represents the experimental contribution of secondary amine (open squares). (Reproduced by permission of Hüthig & Wepf Verlag.)

The activation energy is 42 kJ/mol, higher than in the case of the previous peak. This could be explained on the basis of the lower reactivity of the secondary amine. In fact, steric hindrance and presumably electron pullout due to electrophilic oxygen attached to the molecular backbone oppose to the addition of the secondary amine. On the contrary, the frequency factor is increased 26-fold and this reflects the increased mobility of the functional groups in the nematic phase. The higher value of the frequency factor could be considered as an indirect evidence of the decrease of viscosity of the reacting medium in the nematic phase. Despite the higher activation energy for the addition of the secondary amine, the ratio k_2/k_1 is approximately 4. The values reported in the literature, ranging from 0.2 and 0.4 are a clear evidence of the increased difficulty of the secondary amine to react with the epoxy groups. In our case, the combination of increased activation energy and of increased frequency factor causes a higher reaction rate for the secondary amine that leads to a speeding up of the reaction as soon as the nematic phase is developed during curing.

Also in the case of longer rigid skeleton molecules, a double peak exotherm was evident at the DSC analysis, if the curing is carried out in a temperature range in which the reaction batch is isotropic. This is the case of curing 6,6'-Bis(2,3-epoxypropoxy)-2,2'-binaphthyl (EPBN, Fig. 17).⁴⁶

Figure 18 reports the DSC trace of EPBN. Two endothermic peaks can be observed. The first one, centered at 240°C, with a transition enthalpy of 33.6 kJ/mol, is ascribed to the melting from a solid to a nematic phase, as indicated by microscopic observation under

Table 4. Times of appearance of nematic phases of epoxy resin based on DOMS at different temperatures. First column: curing temperature; second column: reaction enthalpy; third column: time of formation of nematic phase observed by optical microscopy; fourth column; position of the first peak maximum; fifth column: position of the second peak maximum; sixth column: time lag of the DSC cell

$T/^\circ\text{C}$	$\frac{\Delta H_{\text{exp}}}{(\text{J/g})}$	$t_{\text{microscopy}}/\text{min}$	$t_1^{\text{max}}/\text{min}$	t_2^{max}	$\tau^{\text{DSC}}/\text{min}$
130	341.9	3.33	1.50	3.07	0.78
140	373.2	2.42	1.17	2.12	0.48
150	370.0	1.88	0.82	1.97	0.34
160	346.8	1.78	0.65	1.57	0.27
170	320.8	1.35	0.63	1.40	0.33
180	340.2	0.67	0.49	1.13	0.25
190	303.9	0.75	0.48		0.30

crossed polarizers; the second peak, centered at 270°C , with a transition enthalpy of 0.50 kJ/mol , can be attributed to the isotropization of the melt, as confirmed also by optical microscopy. The low value of the enthalpy related to the second peak is indicative of a transition from a nematic to an isotropic state.

EPBN was cured with 4,4'-diaminodiphenyl sulphone (DDS) in the DSC pan, both in dynamic and isothermal conditions. DDS is a typical amine curing agent for high performance conventional epoxy resins. Figure 19 reports the dynamic scan of the EPBN-DDS mixture during reaction. Mixing EPBN with DDS results in lowering the mixture melting point, thus allowing the reaction to start at 200°C , as can be inferred from the DSC scan. At about 270°C the cure is complete, as it can be deduced from an analysis of the second heating scan where the absence of exotherms indicates no post-cure in the resin. A network having a liquid crystalline structure is obtained, as indicated by the textures observed by microscopy under crossed polarizers. Furthermore, X-ray analysis performed on the cured samples showed the typical nematic halo. In spite of its kinked geometry, DDS can promote the alignment of the prepolymeric chains, leading therefore to networks with liquid crystalline order. A second dynamic DSC scan, performed on the cured sample, reveals the T_g at 254°C . In the case of conventional epoxy resins cured with DDS, lower T_g s resulted. In fact, even in the case of a tetraglycidyl epoxy resin, tetraglycidyl-4,4'-diaminodiphenylmethane, for which a higher crosslink density is expected, lower T_g results for the monomer cured with DDS.⁴⁷

The isothermal reaction of the EPBN-DDS mixture was carried out at 250°C . A double exothermic peak can be observed (Fig. 20). We have already pointed out that this peculiar shape of the peak indicates a change of the rate of reaction, connected with the growth of a

Table 5. Kinetic parameters associated with the first exothermic peak. First column: curing temperature; second column: reaction enthalpy; third column: activation energy; fourth column; pre-exponential factor; fifth column: reaction order; sixth column: reaction order; seventh column: kinetic constant

$T/^\circ\text{C}$	$\frac{\Delta H}{(\text{J/g})}$	$\frac{E_a}{(\text{kJ/mol})}$	$\ln k_0$	m	n	K_1
150	268.8	35.10	10.05	0.284	0.993	1.07
160	275.4					1.35
170	255.6					1.68

Table 6. Kinetic parameters associated with the second exothermic peak. First column: curing temperature; second column: reaction enthalpy; third column: induction time; fourth column: activation energy; fifth column: pre-exponential factor; sixth column: reaction order; seventh column: reaction order; eighth column: kinetic constant; ninth column: ratio between kinetic constant related with second and first peaks

$T/^\circ\text{C}$	$\frac{\Delta H}{(\text{J/g})}$	τ/min	$\frac{E_a}{(\text{kJ/mol})}$	$\ln k_0$	m	n	K_2	K_2/K_1
150	101.2	0.71	41.50	13.30	0.904	1.997	4.47	4.17
160	71.0	0.60					5.88	4.35
170	65.0	0.54					7.62	4.53

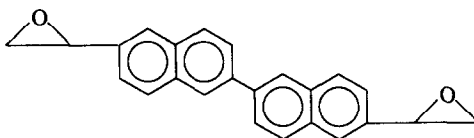
nematic prepolymer when the starting components are not liquid crystalline themselves. Therefore the double peak observed in this case looks incoherent, as EPBN is in its nematic phase in the range of temperature of the hardening reaction. This discrepancy can be explained by observing the EPBN-DDS mixture under optical microscope: at 250°C the blend of the two components is indeed isotropic, and only after one minute of reaction at this temperature the liquid crystalline order appears. Therefore, also for this system the reaction rate changes after the mesophase occurs.

Figure 21 reports the thermogravimetric analysis performed on the network obtained curing EPBN with DDS at 250°C. Decomposition of the resin begins near 340°C. The high value of the decomposition temperature can be ascribed to the presence of the binaphthyl group as rigid block which strongly enhances the thermal stability of the material.

4. LIGHTLY CROSSLINKED LCER

Esterified epoxies are the product of the reaction between epoxy resins and carboxylic acids. Their application, in the case of commercial epoxies, lies in the field of adhesives, casting and laminates.⁴⁸ When fatty acids are used to esterify epoxies, products which are somewhat similar to alkyd resins are obtained. The reaction can be summarized by the steps reported in Fig. 22. The first reaction involves the opening of the epoxy ring by the carboxylic group. The resulting hydroxyl group is subsequently involved in the crosslinking reaction, which can take place either through the formation of ester linkages by condensation with excess carboxylic acid molecules, or, in the presence of catalytic amounts of proton donors, through homopolymerization with epoxy molecules not yet reacted.⁴⁹

The resulting networks generally exhibit low crosslinking density. When the reaction is therefore carried out between a mesogenic epoxy molecule and an aliphatic diacid, an



EPBN

Fig. 17. Molecular formula of EPBN.

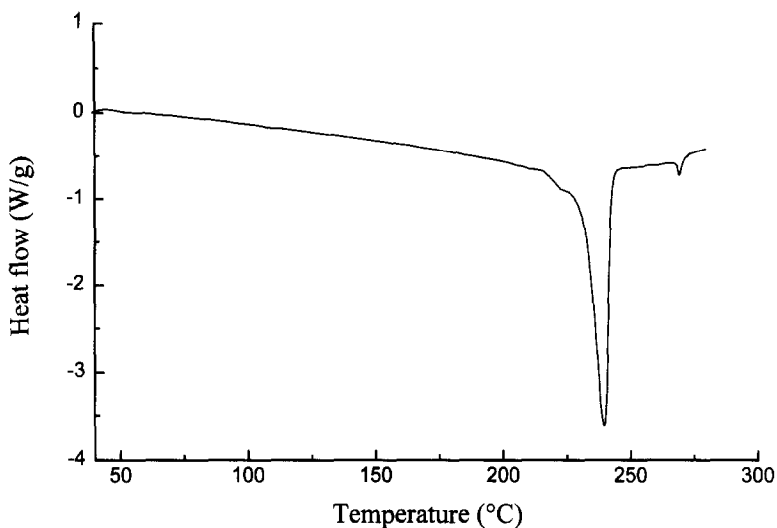


Fig. 18. DSC curve of EPBN. Heating rate 10°C/min. (Reproduced by permission of Hüthig & Wepf Verlag.)

anisotropic thermoset can result. It has been proposed⁵⁰ to consider these systems as highly viscous liquids in the liquid crystalline phase; they are therefore expected to exhibit phase transitions. It was reported⁵¹ on the synthesis and thermal characterization of networks prepared from epoxy endcapped oligoethers, based on 4,4'-dihydroxy- α -methylstilbene and α,ω -dibromoalkanes, cured with aromatic diamines. The same authors⁵² discussed the

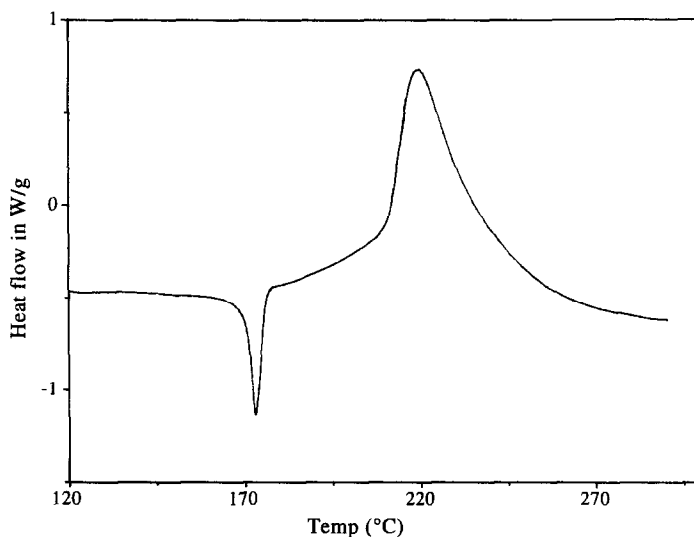


Fig. 19. DSC curve of EPBN-DDS mixture. Heating rate 10°C/min. (Reproduced by permission of Hüthig & Wepf Verlag.)

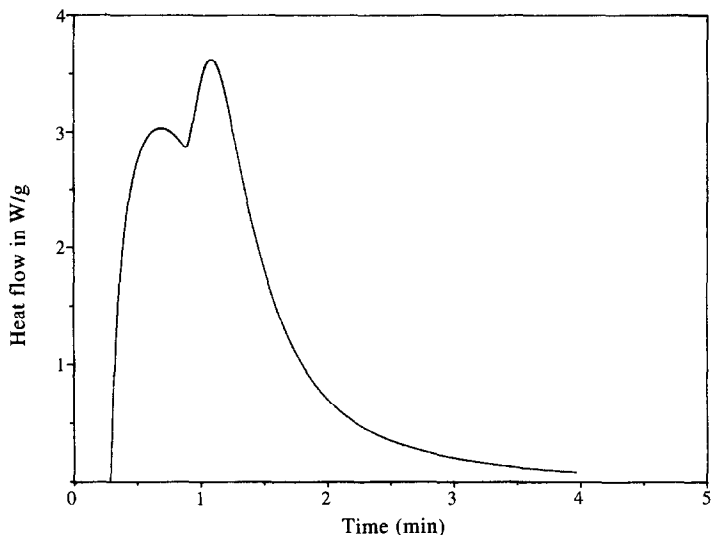


Fig. 20. DSC isothermal scan at 250°C of EPBN-DDS mixture. (Reproduced by permission of Hüthig & Wepf Verlag.)

orientation achieved by processing these materials under tensile stress and in applied magnetic fields. The first approach was successful in the case of the less crosslinked networks, but a good orientational stability above T_g was achieved only for higher crosslinking density obtained by curing the material under magnetic fields.

The features of networks obtained by reacting at 180°C the previously reported compound

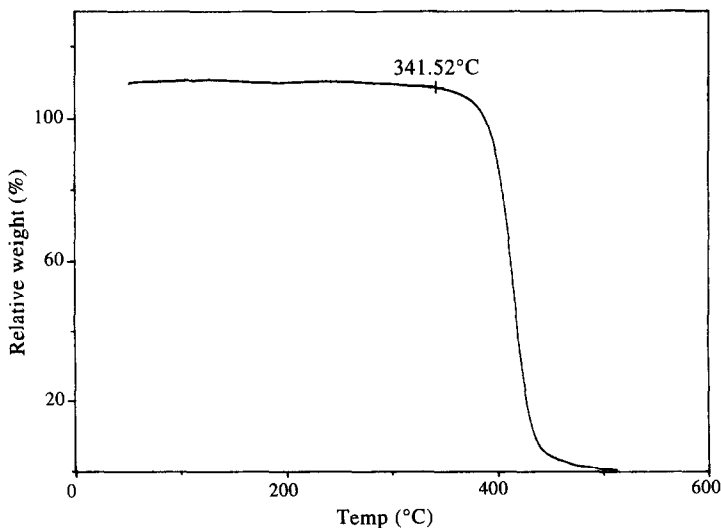


Fig. 21. TG scan of EPBN cured with DDS at 250°C. Heating rate 10°C/min. (Reproduced by permission of Hüthig & Wepf Verlag.)

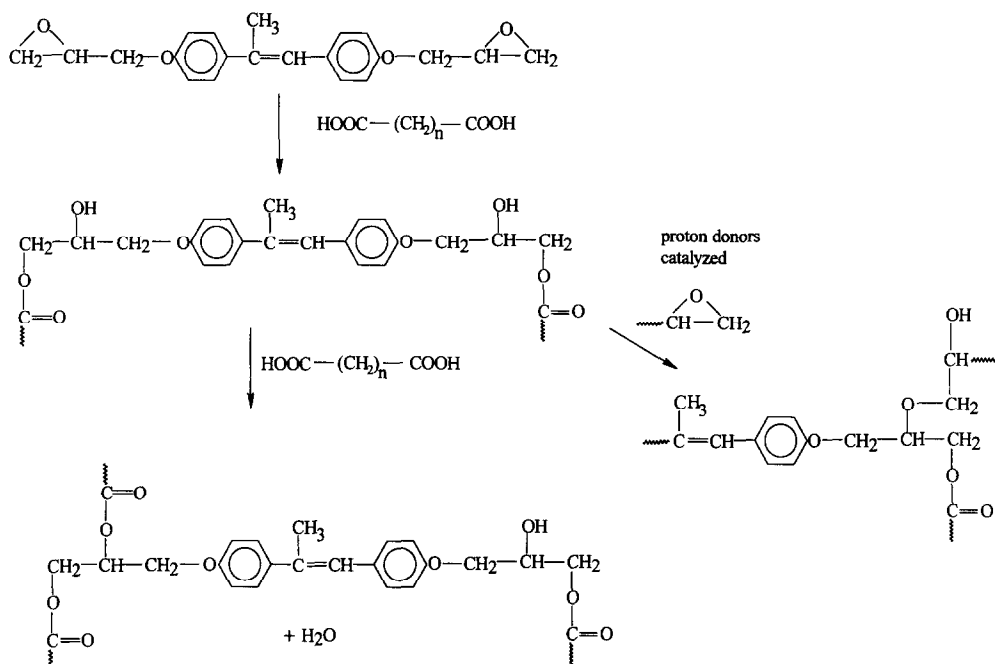


Fig. 22. Reaction scheme of epoxy resins and dicarboxylic acids.

DOMS with stoichiometric amounts of aliphatic diacids $\text{HOOC}-(\text{CH}_2)_n-\text{COOH}$, with n ranging between 2 and 8, were examined by the authors. In all cases a liquid crystalline network was obtained. The characteristics of these materials are summarized in Table 7. For $n = 2$ the material exhibits a nematic phase, while all the other acids gave smectic materials, as shown by X-ray analysis. It has been already reported in the literature that network formation in the mesomorphic state leads not only to the "freezing in" of the structure developed in the early stage of polymerization, but can also produce an ordered polymer. Nematogenic monomers can therefore yield a network with smectic ordering. This experimental evidence was also found in the case of networks obtained from difunctional acrylate monomers,⁵³ from triazine monomers⁵⁴ and from epoxy oligomers.⁵¹

In our case, however, a biphasic system was obtained, as shown by the presence of weak crystalline reflections in the X-ray pattern. In some cases, i.e. for $n = 5$ and 8, crystallinity was slowly developed only by annealing the samples at room temperature for months. This is made possible by the low values of T_g s, ranging around room temperature, for these networks. In order to properly characterize the materials, all the samples were annealed at 50°C for 72 h.

In Fig. 23 the isotropization and anisotropization temperatures, as revealed from optical analysis under crossed polarizers and from DSC analysis, are reported. An odd-even effect can be shown for all the three sets of values. In the case of even n , higher transition temperatures are obtained. This was also reported in the case of semiflexible mesophasic polymers having α -methylstilbene as rigid core and aliphatic spacers of different length.⁵⁵

Table 7. Characteristics of the materials obtained by curing at 180°C DOMS with carboxylic acids of general formula $\text{HOOC} - (\text{CH}_2)_n - \text{COOH}$

n	Mesophase exhibited	T_g (°C)
2	N	49
3	S	29.5
4	S	33
5	S	30
6	S	26
7	S	31.4
8	S	29.5

It was shown⁵⁶ that in the case of side-chain LC polymers, the flexible segments mainly act as spacers between the main-chain and the side mesogenic groups, thus allowing the assembling of the material in anisotropic structure. A similar role is also played by the flexible segments connecting the mesogenic groups in the case of a main-chain LC polymer. Theoretical calculations^{57,58} showed that also in low molecular weight liquid crystals the flexible segments are not simply space fillers, but take part to the anisotropy of the phase. Therefore, it is not surprising that also in the case of a lightly crosslinked LC network, the

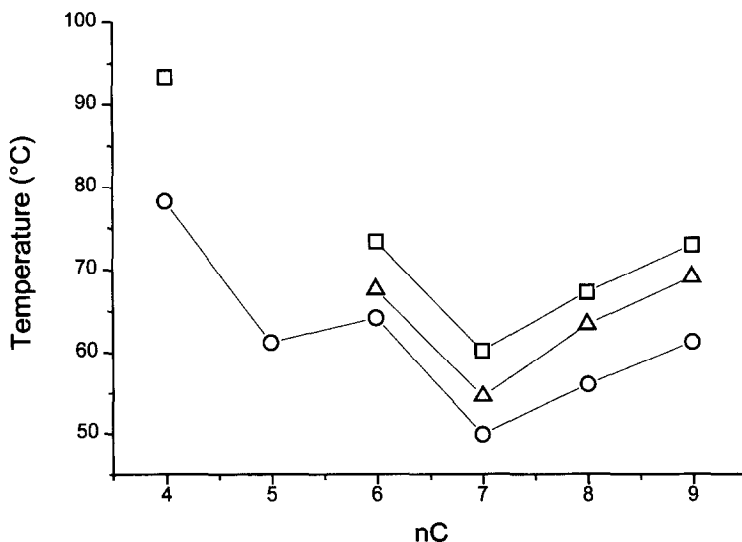


Fig. 23. Anisotropization temperature (○) and isotropization temperatures from I (□) and II (Δ) DSC scan vs carbon atoms number of carboxylic acids for networks obtained by curing DOMS with $\text{HOOC}(\text{CH}_2)_n\text{COOH}$ at 180°C. For $n = 4$ and 5 some data could not be determined.

aliphatic portion plays an active role in the development and in the stabilization of the mesophase.

Figure 24 reports a typical DSC scan for such a material. As it can be seen, a wide endotherm, due to both the overlapping of melting and isotropization peaks, is present. This feature made calorimetric analysis inadequate in order to evaluate the isotropization enthalpy and entropy.

In Fig. 25 the spacings corresponding to the distance between two smectic layers of the different networks are reported. There is a small increase of the spacing from 12.4 to 15.1 Å, as expected as a consequence of the increasing length of the acids. In the case of linear thermotropic polymers giving a smectic phase, the increase of spacing with the length of the flexible aliphatic spacer was ascribed to the bigger distance between the smectic layers.⁵⁹

Poorly crosslinked networks have recently been the object of many experimental and theoretical investigations. Their interest lies in fact in the ease of orientation and the resulting change in optical properties,⁶⁰ which make them attractive in the field of non-linear optics (NLO). Many theoretical predictions have been proposed, since the formulation of the Landau-de Gennes theory for the behavior of LC elastomers under mechanical stress.⁶¹⁻⁶⁴

The possibility of orienting our materials by stretching above T_g , and freezing the obtained orientation by quickly cooling the samples to room temperature⁶⁵ was considered. Our attention was focused on the network obtained by reaction between DOMS and the acid having $n = 8$, i.e. decanedioic acid (SA).

Figure 26 reports the DSC graph for fully cured DOMS-SA system. From the graph, a T_g of 27°C can be inferred. The endotherm centered at 81°C with $\Delta H = 17.8$ J/g was ascribed to the isotropization of the sample, as revealed also by optical observation; however, the high enthalpy value may be due also to the melting of crystalline portions developed in the sample by effect of annealing. As we have already explained, this material exhibits a smectic phase.

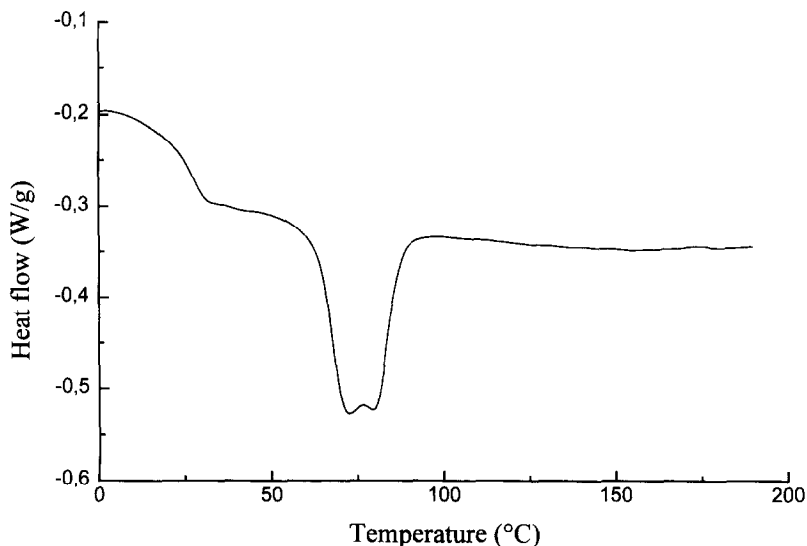


Fig. 24. DSC scan for a network obtained by curing DOMS with $\text{HOOC}(\text{CH}_2)_n\text{COOH}$ at 180°C.

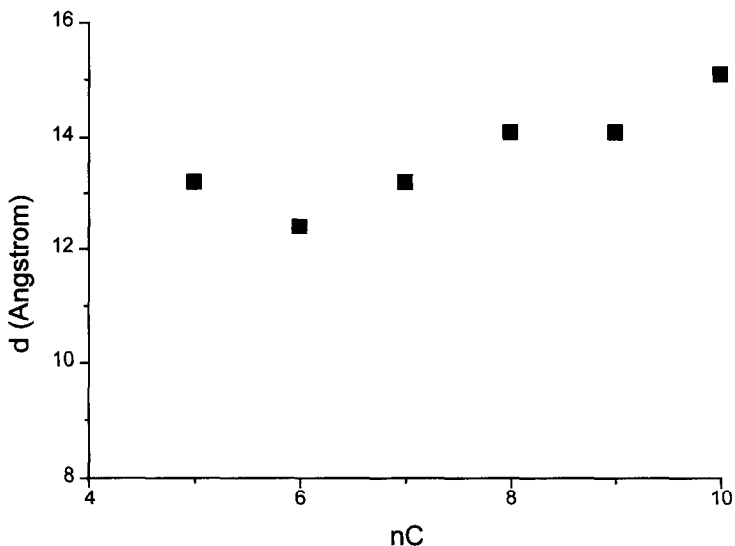


Fig. 25. Spacing of the smectic layers as obtained from X-ray diffraction patterns vs carbon atoms number of carboxylic acids for networks obtained by curing DOMS with $\text{HOOC}(\text{CH}_2)_n\text{COOH}$ at 180°C .

A DOMS-SA film was stretched at 35°C up to $\lambda = 1.8$ (where λ is defined as $(l - l_0)/l_0$ with l_0 initial sample length and l = sample length after stretching). From a macroscopic point of view, the sample turned from turbid and white to transparent. The optical micrography of this sample (Fig. 27) indicates a transition from a multidomain texture to a monodomain. The

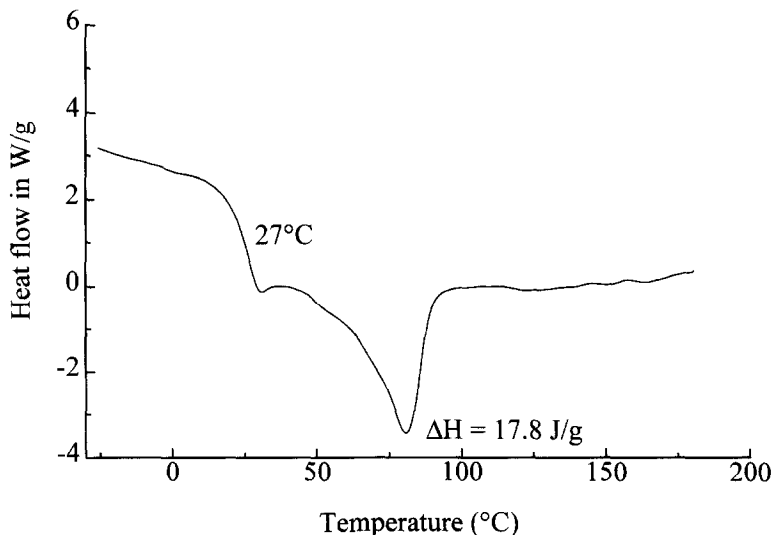


Fig. 26. DSC graph of cured DOMS-SA system. (Reproduced by permission of Hüthig & Wepf Verlag.)

stretched sample is in the upper part of the picture, while the bottom portion is almost unstretched. The lower region exhibits a variegated texture, typical of a polydomain liquid crystalline structure. The situation is completely different for the upper portion: in this case a homogeneously coloured alignment can be observed under crossed polarizers, which is indicative of polymer orientation in a monodomain.

The X-ray pattern performed on the oriented network (Fig. 28) shows a broadened wide angle reflection at the equator. The smectic layer reflections are visible at the meridian: this evidence can be explained on the basis of the orientation of the smectic layers orthogonal to the direction of stretching. Similar results were also found in the case of highly stretched fibers of a smectic main-chain elastomer.⁶⁶

The calculation of the order parameter from the X-ray pattern of liquid crystalline materials has been extensively discussed in the literature.^{67,68} In our case, S was calculated from the following equations:

$$S = \frac{1}{2}(3\langle \cos^2\Theta \rangle - 1)$$

$$\langle \cos^2\Theta \rangle = 1 - 2\langle \cos^2X \rangle$$

$$\langle \cos^2X \rangle = \frac{\int_0^{\Theta/2} I(\cos^2X)(\sin X)dx}{\int_0^{\Theta/2} I(\sin X)dx}$$



Fig. 27. Optical micrography under crossed polarizers at room temperature of a DOMS-SA film stretched at 35°C up to $\lambda = 1.8$ and rapidly cooled down to the glassy state. (Reproduced by permission of Hüthig & Wepf Verlag.)

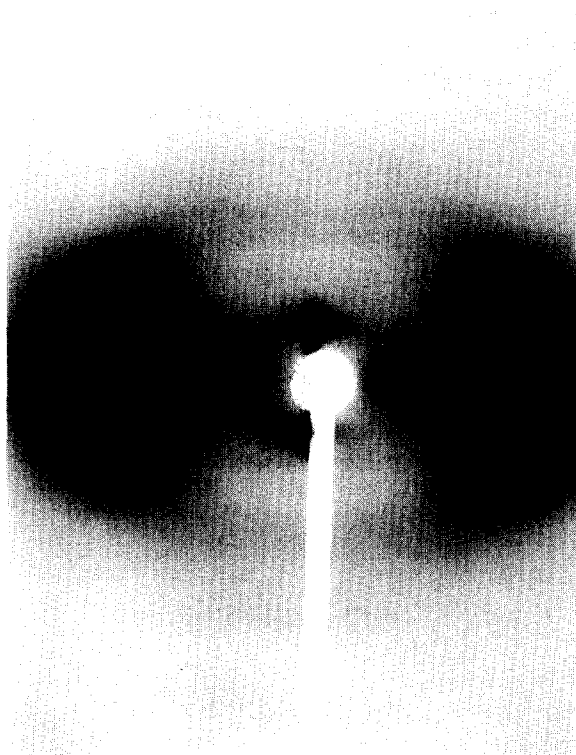


Fig. 28. X-ray diffraction pattern at room temperature of DOMS-SA film stretched at 35°C up to $\lambda = 1.8$ and rapidly cooled down to the glassy state; stress direction vertical. (Reproduced by permission of Hüthig & Wepf Verlag.)

where X is the coordinate of an azimuthal scan on the X-ray pattern. In the case of the previously discussed stretched sample, a value of 0.8 was calculated for the order parameter. This evidence shows that very high orientation can be obtained for this material, and makes it very promising in the field of optical applications.

DOMS-SA films were investigated by thermomechanical analysis. The samples were subjected to a constant force and their dimension change was monitored while temperature was increased at a constant rate of 5°C/min. Fig. 29 reports a typical plot relative to these experiments. The curve (a) refers to an unstretched sample exhibiting therefore a multi-domain structure. The small slope discontinuity in the first part of the curve is due to onset of T_g , which causes of course a change of the thermal expansion coefficient α . The subsequent steep slope increase up to about 88°C, followed by a sudden dimensional fall, is intriguing and requires a proper interpretation. In the case of a previously oriented sample [Fig. 29(b)] no peak could be detected at all, and the trend of $\Delta l/l_0$ vs temperature only exhibits a sharp fall at 85°C. We related therefore the presence of the peak, in the first case, to the orientation of the sample subjected to load in the rubbery anisotropic state, which is then followed by an abrupt longitudinal shrinkage at the isotropization. This can be explained on the basis of the more extended conformation which the polymeric chains are forced to assume

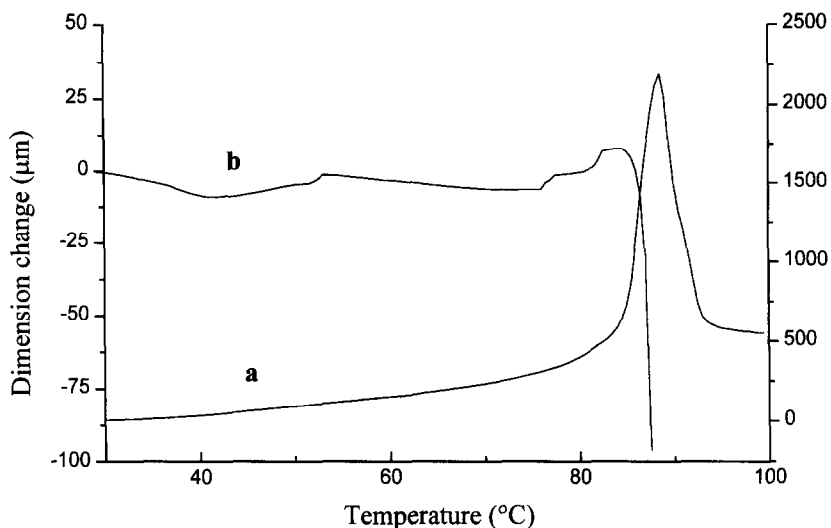


Fig. 29. Thermomechanical analyses performed on DOMS-SA system; dimension change vs temperature. Unstretched sample (curve a, right Y axis); previously stretched sample (curve b, left Y axis). Heating rate 5°C/min.

in the LC oriented state, when the rigid-rod portions are aligned in a smectic structure. In the case of the oriented sample, no additional extension can be induced by the applied stress, and the only detectable phenomenon is the shrinkage as a consequence of the chains coiling configuration at the isotropization. We concluded, therefore, that the peak maximum temperature could be related to the isotropization temperature of the samples under mechanical stress.

Figure 30 reports the peak maximum temperature vs $\Delta l/l_0$, the sample relative elongation. Different values of $\Delta l/l_0$ were obtained by performing thermomechanical experiments at different values of the applied force. As it can be inferred from the diagram, isotropization temperature increases from about 80 to about 90°C with increasing the elongation. If we assume that, as we stated before, the elongation is related to the sample orientation, then this experimental trend can be considered an evidence of the mesophase stabilization due to the mechanical field applied. Similar results were found by Kaufhold et al.⁶⁹ in the case of side-chain nematic elastomers. In their case, the phase transformation temperature T_{NI} is shifted of 7.5K by the maximum applied stress. These results are in agreement with the Landau-de Gennes theory,^{61,62} which predicts a displacement of the clearing point to higher temperatures in the presence of an external mechanical field.

In order to investigate how the reaction between DOMS and SA could lead to different products as a consequence of the different molar ratio of the two components, the two monomers were reacted also in different stoichiometric ratios, ranging from 0,22:1 to 0,80:1 SA/DOMS. The characteristics of the resulting products are shown in Table 8. In the case of the 0,79 SA mixture, an incomplete gelation resulted. In all other cases, no network was formed, but only fluid mixtures of increasing viscosity in correspondence of increasing amount of acid.

Molecular weight per epoxy (WPE) and molecular weights have an increasing trend as

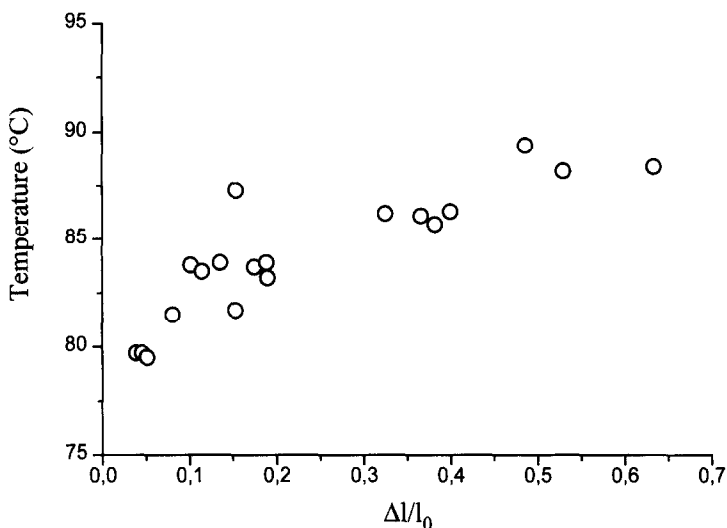


Fig. 30. Peak maximum temperature obtained from thermomechanical analysis vs $\Delta l/l_0$ for DOMS-SA films.

expected. The anomalously low value of molecular weight in the case of the 0,79 product can be ascribed to the poor solubility of this sample in chloroform during phase vapor osmometry experiments.

X-ray experiments were performed at room temperature on these samples; for each material, but the one corresponding to 22% SA, which resulted crystalline, both nematic and smectic reflections could be observed in the diffraction pattern.

The effect of the reaction on the mesophase stabilization is evident. DOMS is a monotropic nematic compound with anisotropization temperature of 68°C; after the reaction with 0,22:1 SA, a crystalline product is obtained with a melting temperature of 51°C and an isotropization temperature of 101°C, as inferred from both DSC analysis and microscopic observation. When DOMS is reacted with increasing content of SA, liquid crystalline enantiotropic oligomers are obtained whose isotropization temperatures are comprised between 98 and 79°C.

Table 8. Characteristics of the materials obtained by curing at 180°C DOMS with SA in different stoichiometric ratios

% SA	WPE (g/eq)	<i>Mn</i>	X-ray	T _g (°C)	T _a (°C)	T _i (°C)
0	182	338	K		68	115
22	341	432	K		100	101
36	504	1331	N + S	14	96	98
50	622	1750	N + S	15	88	89
61	1467	2035	N + S	12.5	78.5	78.8
79	1875	1627	N + S	16,8	93	94

5. ORIENTATION OF LCER

LCER, as a class of liquid crystalline thermosetting resins, offer the unique possibility of exploiting the properties of both low and high molecular weight materials. The cured sample, in fact, can be regarded as a crosslinked network, whose structure is reminiscent of the liquid crystalline order before gel point is reached, but it is not any longer able to undergo to any viscous deformations.⁷⁰⁻⁷² The crosslinked tridimensional structure can exhibit high modulus and high glass transition temperatures, being suitable for the production of composite structure for advanced application,^{73,74} or elastic behavior featuring low modulus and high toughness. The main feature affecting the phase transitions is the degree of crosslinking produced during the curing reactions. If the degree of crosslinking is very high, then the molecular structure is fixed quite tightly. The molecular conformations cannot be rearranged freely and the liquid crystalline structure is stabilized over a wide temperature range. As a result, the clearing point of the sample cannot be reached and the birefringence is observed until the thermal decomposition of the matrix takes place. On the contrary, if the crosslinking density is low and the network is not rigid enough to prevent the phase transitions, the clearing point of the material is detected upon heating. In fact, the chemical bonds connecting the mesomorphic rigid blocks are flexible enough to allow wide conformational motions that determine the phase transition to the isotropic state by increasing the temperature. However, the tridimensional network structure is preserved and the former structure is recovered as the temperature is decreased below the isotropic-liquid crystalline transition.

If the crosslinking reactions are stopped before the achievement of the gelation point, i.e. the point that indicates the initial formation of the tridimensional network that hinders any viscous deformation, the mixture is composed by linear or branched molecules. The viscosity of the material at this stage is mainly governed by the average molecular weight, and the usual behavior of low mass liquid crystals can be observed for what concerns their orientation.⁷⁵⁻⁷⁷ If the liquid crystalline resin is not subjected to external fields the domain directors are randomly oriented in the space and the overall order parameter is very low. But if mechanical or electromagnetic fields are applied to the sample in the liquid crystalline state, an easy orientation of the domains along a preferred direction is achieved. The subsequent crosslinking reaction locks the molecules in the aligned conformations achieved under the influence of the external field and stabilizes the structure exhibited at the gel point. This procedure can be used for the production of highly aligned samples that retain the molecular structure also after the removal of the external field that has been used for the macroscopic orientation. The alignment of the rigid molecular backbone remains then stable over a wide temperature range.^{51,52}

The processing of a low viscosity epoxy/curing agent mixture has been reported for the preparation of uniformly crosslinked and oriented liquid crystalline thin films.

The liquid crystalline epoxy networks have been aligned either by an elongational flow or by a magnetic field. The first method is used to align the network with a low crosslinking density above the glass transition temperature. On cooling below the T_g , the orientation was frozen into the glassy state and the sample retained its extended form. This process closely resembles the drawing procedure of thermoplastics to produce oriented fibers or films with anisotropic properties. The difference is in the degree of orientation that can be achieved in the two different cases. In fact, while during the drawing of isotropic thermoplastics or the extension of lightly crosslinked thermosets the molecules relax back to the equilibrium

conformation very quickly and the stresses frozen into the matrix to achieve a significant orientation are very high, in the second case the liquid crystalline nature of the material greatly encourages the alignment of the molecules along the drawing direction. Consequently the stresses frozen in the material are lower and this result in an increase of dimensional stability. As the crosslinking density was increased more energy was required to orient the sample mechanically. The order parameter of the mechanically oriented sample, measured by means of X-ray diffraction patterns, indicates values of approximately 0.5 achieved with an extension ratio of 2.0.

In order to improve the molecular orientation along a preferred direction the LC phase had to be aligned during the crosslinking process. To fulfill this requirement the sample was cured under the influence of a strong magnetic field (13.5 Tesla). Strong magnetic fields applied to small liquid crystalline molecules or to linear polymers cause the alignment of the domains along the field direction and produce oriented macrodomains. Order parameter as high as 0.6 were obtained if the samples were cured under the influence of strong magnetic field.

Mechanically oriented sample will of course lose their orientation upon heating above T_g . The sample shrinks back to the equilibrium conformation relaxing the stresses frozen in the matrix. On the other hand, for the highly crosslinked samples cured in the magnetic field the orientation can be locked in by the crosslinking and a stress-free matrix is obtained. Therefore, no dramatic dimension changes are detected heating the sample above the glass transition temperature.⁵²

Nevertheless, a very effective method to achieve uniform molecular alignment in the liquid crystalline materials seems to be the liquid crystal–surface interactions which can be combined with an applied electric field or with unidirectional shear flow. This process can be used to obtain film with a thickness of few ångstrom, while for the obtainement of thicker samples the stretching procedure seems to be preferred.

LCER obtained by mixing the stoichiometric amount of epoxy precursor and an aromatic amine is suitable to be used for the preparation of uniformly planar aligned thin film. In particular, the case of DOMS cured with DAT has been reported.

The processing of the liquid crystalline resin to produce the oriented film closely resembles the step for the production of optical cells. In fact the epoxy resin is oriented during the curing reaction by means of the surface–liquid crystalline interaction. The liquid crystalline material is supported between aligning substrates, and when the uniform orientation is achieved in the film the crosslinking reaction is promoted in order to permanently stabilize and lock in the achieved orientation.

In order to accomplished this result satisfactorily, the mechanism and kinetics of curing reaction has to be investigated and extensively characterized.

In particular the reduction of the reaction rate allows the obtainement of better oriented sample. In fact, the reorientation of the molecules along a common direction and the formation of the uniform domain is greatly favored if the viscosity of the liquid crystalline phase is low. This requirement is fulfilled at the beginning of the crosslinking reaction, due to the low molecular weight of the reacting molecules. As the reaction produces longer molecules, the viscosity increases dramatically. A threshold value is eventually reached when further orientation of the molecules is virtually hindered. It is particularly important that the desired molecular orientation is achieved before this limit is reached. The reaction of epoxy group with aromatic amines is catalyzed by traces of acids or alcohol or water.^{40–42} Therefore the use

of carefully purified chemicals enabled the authors to successfully slow down the reaction rate and to obtain uniformly oriented samples.

As an aligning layer, the deposition of evaporated metals or oxides (i.e. silicon monoxide) at oblique incidence is a common practice in the preparation of electrooptical devices.⁷⁸⁻⁸¹ Many processing parameters affect the structure of the evaporated silicon monoxide, and thus the surface-liquid crystalline interaction. The possibility of selecting different direction for the evaporation source provides aligning substrates with different tilt angle of the silicon monoxide crystal with respect to the glass substrate surface. The effect of different tilt angle on the orientation of the liquid crystal is not straightforward. Depending on the properties of the specific liquid crystalline molecules different orientation are obtained in the LC film. The fine and flawless texture obtained is available for the preparation of defect free cells with uniform alignment of the liquid crystal. The drawbacks of this technique are both technical and economical. In fact, the processing cost is high and the production rate low. The dimension of the treated substrate is limited by the necessity of assuring uniform incident angle along the whole sample.

However, in the industrial practice the most widely used aligning technique is the deposition of thin polymeric films and their subsequent mechanical orientation.⁸²⁻⁸⁹ Many polymers are available as aligning layer. The use of polyvinylalcohol, polyamides, polyesters and polyimides have been reported. The polymer is dissolved in a suitable solvent and the solution spin coated on top of the glass substrate. The concentration of the solution is not critical and the spinning parameters can be adjusted in order to produce a very thin and uniform layer. In the case of polyimides as aligning layer, a curing reaction is frequently necessary to crosslink the polymer onto the glass substrate.⁹⁰

After the polymeric film has been properly obtained, it is oriented along the preassigned direction by mechanical rubbing or buffing. It is widely acknowledged that the rubbing mechanism produces local change in the polymer structure, such as molecular reorientation and shearing. It also produces microgroves.⁹¹ The distribution of polar groups on the polymer surface is affected by rubbing. As a result, the rubbing technique has been reported to affect greatly the tilt angle of the liquid crystalline molecules with respect to the polymeric surface. Even though many recent publications are available about the aligning surface-liquid crystalline interaction, the orienting mechanism is still lacking in complete understanding. It is widely accepted that the molecular orientation at the surface affects the liquid crystalline phase, but scratches and micro groves produced on the surface are not important. However, the rubbing process produces dust and electrostatic charges. The defects produced in the liquid crystalline structure is therefore a serious drawback of the rubbing procedure.

The mixture composed by DOMS and DAT has been used for the preparation of a thin LCER film with uniform planar orientation. The thickness of the film is controlled by placing spacers between the glass substrates supporting the epoxy mixture. A rubbed polyimide coating is used to achieve the alignment of the epoxy film. The mixture is melted on the glass substrate at the temperature of 140°C, and the cell is subsequently sealed placing another glass substrates with the rubbing directions of the polyimide substrates parallel to the previous one. Then the temperature is lowered to 110°C to allow the curing reaction to take place. The interactions between the orienting surface and the reacting mixture greatly stabilize the liquid crystalline phase, delaying the crystallization of the mixture. As a result, the curing kinetics is slowed down, allowing the molecules to orient along the rubbing direction.

Although the mixture does not exhibit the liquid crystalline behavior when the parent compounds of the blend are melted, the nematic phase appears during the curing process. The epoxy and the curing agent are in the isotropic state after melting, and the fractional conversion is virtually zero. After the reaction starts and proceeds further on, the fractional conversion and the average molecular weight of the epoxy resin increase. It was reported that the reaction of the primary amine with the epoxy compound is favored with respect to the secondary one. The primary reason for this behavior is due to the increased steric hindrance caused by the addition of the first epoxy group to the nitrogen atom. This accounts for the formation of linear or slightly branched oligomers. The aspect ratio of the molecules increases and the liquid crystalline phase is stabilized by intermolecular forces. As a result of formation of oligomers, the initially isotropic state transforms into nematic phase. The appearance of the birefringent nematic phase was observed by polarizing microscope.

The following picture sequence (Fig. 31), recorded at the temperature of 80°C, illustrate the curing process taking place when the sample is supported between aligning layers. The DOMS and curing agent system is in the isotropic phase immediately after melting. The small aspect ratio of the DOMS molecule does not allow the appearance of the liquid crystalline phase. After the initial stage of the curing phenomena birefringent domains form into the isotropic melt. The domains are randomly oriented at first. As the domain size increases and they merge into a continuous liquid crystalline phase, the orientation transmitted by the aligning layer starts to control the LCET orientation.

The overall orientation achieved at the end of the curing reaction and locked into the molecular network is strongly affected by the reaction kinetics.²⁸ In fact, the aligning process is very slow and takes place in the range of several minutes. The viscosity of the reacting mixture during this time has to be low enough to allow the liquid crystalline molecules to arrange along the rubbing direction. As the reaction proceeds further on and the viscosity

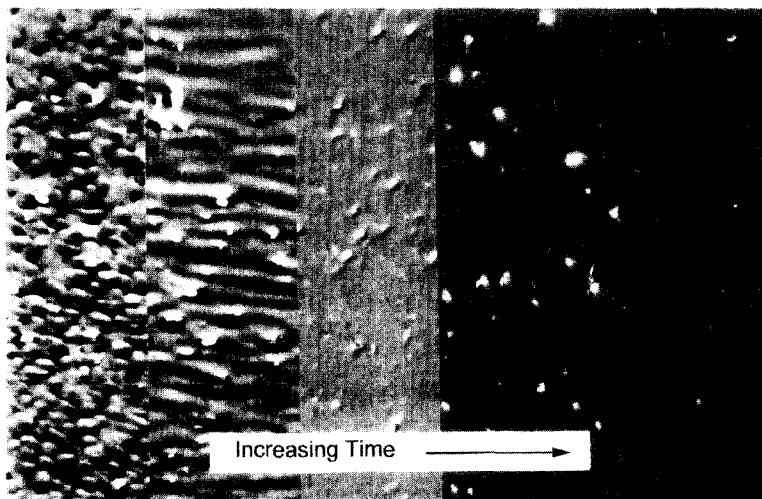


Fig. 31. Sequence of optical micrographs of DOMS-DAT supported between glasses spin-coated with polyimide and unidirectionally rubbed. The picture illustrate the curing process and corresponds to the time sequence recorded at 80°C.

increases due to the higher molecular weight, the molecular motions are hindered. In fact, if the reaction rate is too fast it is not possible to achieve uniformly oriented samples.

If the sample is oriented and cured in the temperature range of the liquid crystalline phase the orientation is locked into a nominally stress-free network and the orientational stability is preserved upon heating of the sample.

Several applications can be designed to take advantage of the permanent orientation achieved in the liquid crystalline thermosets. The preparation of very thin polarizers can be achieved by dissolving the suitable die into the LCET and then curing the matrix in the uniformly oriented planar state. Also the use as potential storage of optical data or as waveguides has been proposed. The strong anisotropy that can be achieved by curing the LCET in the oriented state can be exploited in many optical application not far to be developed. The mechanical properties are more difficult to be exploited, because it is difficult to achieve sufficiently uniform orientation in thicker samples. The difference in mechanical properties between parallel and perpendicular orientation with respect to the molecules could determine some drawbacks to the use of this material as matrix for advanced application composites. In fact it is well known that the very oriented liquid crystalline material exhibits poor mechanical properties in the transverse direction. The material is more brittle and the modulus and strength will be not satisfactory. On the other hand, the coefficient of thermal expansion has been reported to be very low for oriented materials and they have been successfully used for the packaging of electronic devices and circuitry. For this purpose the LCET seems very suitable indeed. In fact, the liquid crystalline polymers are claimed to be very resistant to aggressive chemical environment. If the outstanding dimensional stability upon heating and the almost negligible shrinkage during curing are taken into account, it is clear that these features can be usefully combined for the electronic packaging application.

6. LCER AS MATRIX FOR POLYMER DISPERSED LIQUID CRYSTALS (PDLC)

PDLC are composite materials consisting of liquid crystal droplets having a size of microns, embedded in a transparent polymer matrix. Such devices are of interest because they can be electrically controlled or switched between relatively translucent (i.e. light scattering or nearly opaque) and relatively transparent (i.e. light transmitting) states. This occurs because liquid crystals have two refractive indexes: an extraordinary refractive index measured along the long axis of the rigid-rodlike liquid crystals, and a smaller ordinary refractive index measured in a plane perpendicular to the long axis. As a result, the droplets strongly scatter light when they are randomly oriented in the matrix and the devices appear translucent (or nearly opaque). By applying either electric field or magnetic field, however, the long axes of the liquid crystal droplets become aligned along the direction of the electro-magnetic field vector and they more directly transmit light.^{92,93}

If the refractive indices of the liquid crystalline material and the polymer matrix are closely matched while in the field-induced, aligned state, the devices appear transparent. Thus, upon the application of an electric or magnetic field, for example, the device switches from a state in which it appears translucent (nearly opaque) to a state in which it appears transparent. Upon removal of the electrical or magnetic field, the device reverts to a translucent (opaque) state.

Devices containing composites of liquid crystals dispersed in a polymer matrix have found

use as light valves, filters, shutters, information displays, architectural glass, windows, among others.

Polymers used in making PDLC composites can be either thermosetting polymers or thermoplastic polymers. The thermosettings undergo a curing reaction during which they turn from a lower molecular weight composition into a higher molecular weight cured thermoset resin by means of heat with or without catalyst, hardeners and modifiers. The temperature needed to accomplish this depends on the time of the reaction, on the catalyst employed, on the relative activities of the complementary functional groups in the precursors, i.e, the general and common knowledge of those skilled in the thermosetting resin art. The thermosetting resin utilized may be any of those known in the art.⁹⁴⁻⁹⁷

Thermosetting epoxy matrices are suitable for use in PDLC composites and are most common resins, but matrices of bismaleidimide, phenolic, polyester, polyimide, are usable in PDLC devices. Other thermosetting resins, such as thermosetting resins from acrylics, polyurethanes are usable in making PDLC composites.

Epoxy resins are probably the most studied, and are a particularly preferred material, in making PDLC compositions. They are convenient to use for several reasons. It is easy to mix epoxy resins having different refractive indexes to produce a matrix with a refractive index precisely matched with the extraordinary refractive index of the liquid crystal.

There is a variety of epoxy resins suitable for use in making PDLC composites. All epoxy resins start with an epoxy precursor that is capable of homopolymerization reaction that is catalytically initiated, or coreacted with complimentary functional compositions such as compounds with active hydrogen groups or other reactive groups capable of reacting with an epoxy resin so to cause the molecular weight of the epoxy resin to increase. The performance of the cured epoxy resin depends on the functionality degree of the resin and the coreactant, the molecular configuration of the resin, the equivalent weight of the epoxy resin and any coreactant prior to reaction and the level of cure of the resin. The coreactant can be a curing agent and/or hardener.

Radiation prepolymers⁹⁷ (UV and EB) find wide applications in the field of PDLC technology.⁹⁸ Radiation prepolymers can be generally summarized as:

1. epoxy acrylates;
2. acrylated oils;
3. urethane acrylates;
4. unsaturated polyesters;
5. polyester acrylates;
6. vinyl acrylics; and
7. polyene/thiol systems.

The aim of prepolymer preparation is to obtain a molecule with residual unsaturation, which, when subjected to certain conditions, will crosslink with other unsaturated molecules, and will be converted from a liquid to a solid, coherent film. Obviously the molecules containing unsaturation must remain stable and unreacted until crosslinking is required.

There are some principles which can be applied to the preparation of most prepolymers. Scrupulously clean and dry apparatus, free of residual peroxide, is essential. One of the major considerations to be born in mind, as radiation curable prepolymers are synthesized, is that, while molecular weight is being built up, mostly by exothermic reactions, the vinyl unsaturation must be prevented from engaging in a free radical addition polymerization. Not only

would gelation result, but the fact that two different exothermic reactions would be taking place at the same time, would mean that excessive heat and pressure could build up within the reactor, causing a potentially dangerous situation. These factors have to be taken into account when large scale production of these prepolymers is set up.

Further uncontrolled exothermic reactions can produce undesirable side products, i.e. in the case of acrylates of Bisphenol A, degradation to toluene and other undesired products occurs at above 240°C with much acrid fuming. For similar reasons, an additional inhibitor must be added to improve shelf life, once processing is complete.

Among the various materials belonging to this family of resins, epoxy acrylates (or methacrylates) can find wide application. They are formed by reaction of an epoxy group with acrylic (or methacrylic) acid. A great variety of epoxy resins, ranging from liquid epoxy resins such as the pure bisphenol A diglycidyl ether, to the solid high melting point ones, can be used for the purpose. This range of epoxy acrylates forms the bulk of the epoxy acrylates currently in use. The major restriction is processing viscosity, and for higher molecular weight resins a diluent must be present.⁹⁹

Epoxy resins are well known for their excellent adhesion, flexibility and chemical resistance. These properties are also found in the cured films made from their acrylates.

Conventional thermosets, including epoxy based thermosets, PDLC composites present certain performance problems related to the polymer matrix such as weaker mechanical properties (i.e. brittleness) and low heat resistance, low electrical resistivity, slow curing times and a low stability range with respect to electrooptical properties. A further problem of conventional PDLC devices is "haze", more accurately defined as the "angular dependence of light transmission". The haze phenomenon is due to the perceived mismatch between the extraordinary refractive index of the liquid crystal microdroplets and the refractive index of the matrix when the viewing direction is different from the orthogonal.

An effort has been made in the art to overcome the problem of the angular dependence of light transmission. This effort involved the utilization of a birefringent liquid crystalline side-chain polymer in the polymer matrix instead of the conventional isotropic matrix.^{100,101} The goal was to produce, in a PDLC device, a birefringent, optically anisotropic matrix wherein the ordinary and extraordinary refractive indexes are matched for the polymer matrix material and the dispersed liquid crystal microdroplets. The crosslinked liquid crystalline thermoset presented in reference 100 is based upon a mixture of a commercially available epoxy resin and a mesogenic single amine curing agent. The resulting thermoset is a side-chain cross-linked polymer and not a main-chain or comb-like thermoset. A problem associated with this approach is related to the use of a curing agent containing a single amine. The use of such a curing agent markedly reduces the extent of crosslinking, which in turn reduces the glass transition temperature and mechanical performance of the resin, with the consequence that the solubility of liquid crystal microdroplets in the matrix after curing is increased. This is a significant disadvantage because of the critical importance of effecting and maintaining complete phase separation in polymer dispersed liquid crystal composites.

It would therefore be desirable to provide a component to the polymer matrix which can improve the mechanical and electrooptical performance properties of the PDLC. The desired component should be compatible with the polymer matrix, should improve mechanical and electrooptical properties of the composite, and should, at least in some embodiments, reduce the haze without compromising the degree of phase separation between the polymer continuous and the liquid crystal discontinuous phases of the composite.

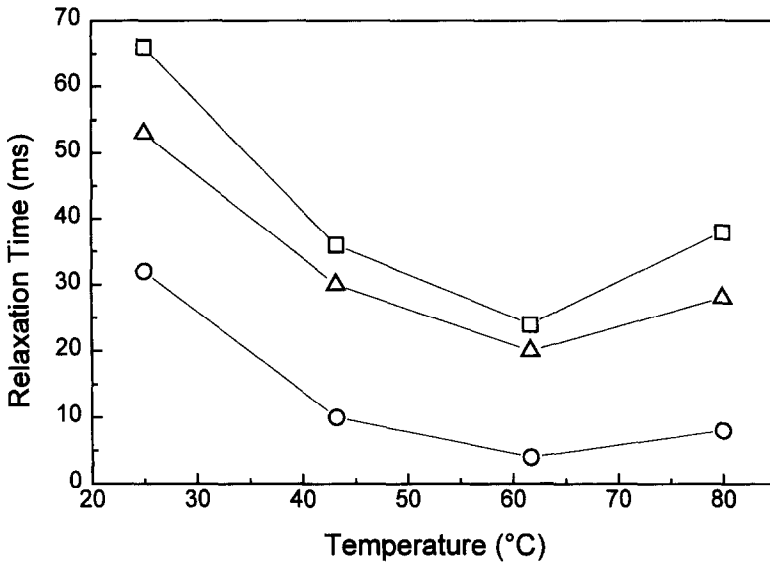


Fig. 32. Temperature effect on relaxation time in standard PDLC films (□); PDLC films containing 40% LCER (Δ), 60% LCER (○).

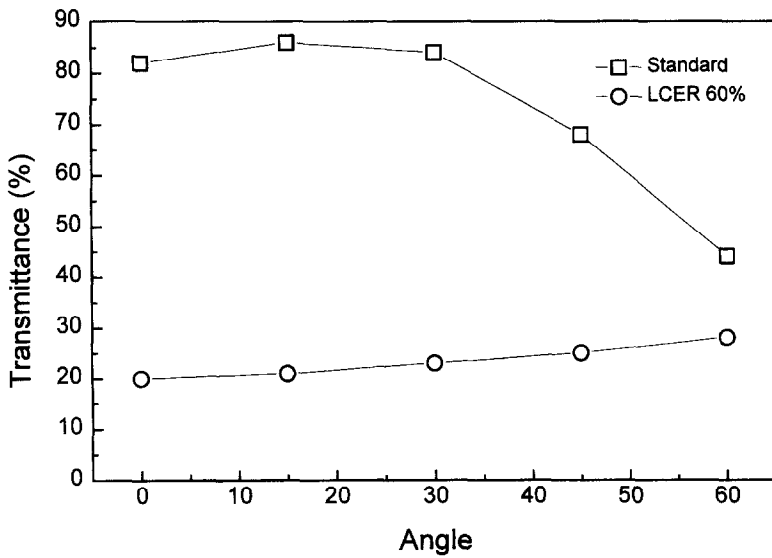


Fig. 33. Angular transmittance for standard PDLC device (□); device containing 60% LCER(○).

Liquid crystalline thermosettable epoxy resins are well known in the scientific literature but they have never been applied to the technology of polymer dispersed liquid crystal composites as main-chain components of the thermoset in the polymer continuous phase matrix. They exhibit enhanced thermal and mechanical properties, as previously discussed. Liquid crystalline epoxy resins may be obtained by endcapping mesogenic or rigid-rod molecules with reactive epoxy groups in the presence of suitable curing agent, typically a diamine. It has been shown that a mesogenic molecular arrangement is sustained over cross-linking reaction when the reaction is performed in the thermal stability range of the liquid crystalline phase.¹⁰² It is further known that the selection of both the glycidyl terminated compound and the curing agent is important to achieve an ordered thermoset and that it is not essential that the epoxy monomer and curing agent form a liquid crystalline phase by themselves.

Figure 32 shows a plot of the temperature effect on relaxation time in standard PDLC film, made with an isotropic epoxy resin, and PDLC film containing different amounts of a liquid crystalline epoxy (DOMS). The relaxation time strongly reduces with increasing percentage of anisotropic resin.

In Fig. 33 the angular transmittance of a PDLC device with 60% liquid crystalline polymer is compared with a standard film having 100% isotropic resin. Aside the low transmittance level of the PDLC sample with 60% liquid crystalline resin, which can be improved by curing the film in electrical field or by surface treatment of the conductive glass, the result of the comparison indicates an improvement of the angular dependence of light transmission of PDLC films. This trend is potentially interesting for developing *index matched controlled* PDLC devices. This evidence confirms the results found by others. In fact, as reported by West,¹⁰³ the use of a liquid crystalline epoxy obtained by curing conventional epoxy resins with mesogenic amines can substantially improve the angular transmission of a PDLC shutter.

REFERENCES

1. Korshak, V.V., *J. Macromol. Sci. Rev. Macromol. Chem.*, 1974, **C11 (1)**, 45.
2. Lee, H. and Neville, K., in *Encyclopedia of Polymer Science and Technology*, Vol. 6, ed. H.F. Mark and N.G. Gaylord. Interscience, New York, 1967, p. 209.
3. Paquin, A.M., *Epoxyverbindungen und Epoxyharze*. Springer, Berlin, 1958.
4. May, C.A. and Tanaka, Y., *Epoxy Resins, Chemistry and Technology*. Dekker, New York, 1973.
5. Stevens, G.C., *J. Appl. Polym. Sci.*, 1977, **21**, 1843.
6. Mika, T.F. and Bauer, R.S., in *Epoxy Resins, Chemistry and Technology*, ed. C.A. May. Dekker, New York, 1988, p. 465.
7. Kinloch, A.J., *J. Mater. Sci.*, 1980, **15**, 241.
8. Kwolek, S.L., US Patent No. 3,671,542, 1972.
9. Roviello, A. and Sirigu, A., *J. Polym. Sci. Polym. Lett.*, 1975, **13**, 455.
10. Jackson, W.J. and Kuhfuss, H.F., *J. Polym. Sci. Polym. Chem.*, 1976, **14**, 2043.
11. Chung, T.S., Calundann, G.W. and East, A.J., in *Handbook of Polymer Science and Technology*, Vol. 2, ed. N.P. Chermisinoff. Marcel Dekker Inc., New York, 1989, p. 625.
12. Finkelmann, H., Meier, W., and Scheuermann, H., in *Liquid Crystals: Applications and Uses*, Vol. 3, ed. B. Bahadur. World Scientific, Singapore, 1992, p. 353.
13. Ophir, Z. and Ide, Y., *Polym. Eng. Sci.*, 1983, **23 (14)**, 792-796.
14. de Gennes, P.G., *C.R. Acad. Sc. Paris*, 1975, **281B**, 101-103.
15. Mueller, H.P., Gipp, R. and Heine, H., Ger. Patent No. 36,22,610, 1986.
16. Dhein, R., Mueller, H.P., Meier, H.M. and Gipp, R., Ger. Patent No. 36,22,613, 1986.

17. Earls, J.D. and Puckett, P.M., Eur. Patent No. 0,379,055 A2, 11/01/90.
18. DeBoer, J.H., *Trans. Farad. Soc.*, 1936, **32**, 10.
19. Houwink, R., *Trans. Farad. Soc.*, 1936, **32**, 131.
20. Morgan, R.J., Mones, E.T. and Steele, W.J., *Polymer*, 1982, **23**, 295.
21. Dugdale, D.S., *J. Mech. Phys. Solids*, 1960, **8**, 100.
22. Rice, J.R., in *Fracture—An Advanced Treatise*, ed. H. Liebowitz. Academic Press, New York, 1968.
23. Morgan, R.J. and O'Neal, J.E., *J. Mater. Sci.*, 1977, **12**, 1966.
24. Morgan, R.J. and O'Neal, J.E., *Polym. Plast. Tech. Eng.*, 1978, **10**, 49.
25. Morgan, R.J. and O'Neal, J.E., *Polym. Eng. Sci.*, 1978, **18**, 1081.
26. Giamberini, M., Amendola, E. and Carfagna, C., *Mol. Cryst. Liq. Cryst.*, 1995, **266**, 9–22.
27. Hikmet, R.A.M. and Broer, D.J., *Polymer*, 1991, **32** (9), 1627–1632.
28. Amendola, E., Carfagna, C. and Giamberini, M., *Macromol. Chem. Phys.*, 1995, **196**, 1577–1591.
29. Apicella, A., Tessieri, R. and de Cataldis, C., *J. Membr. Sci.*, 1984, **18**, 211.
30. Weinkauff, D.H., Kim, H.D. and Paul, D.R., *Macromolecules*, 1992, **25**, 788.
31. Chiou, J.S. and Paul, D.R., *J. Polym. Sci., Part B: Polym. Phys. Ed.*, 1987, **25**, 1699.
32. Weinkauff, D.H. and Paul, D.R., *J. Polym. Sci., Part B: Polym. Phys. Ed.*, 1991, **29**, 329.
33. Weinkauff, D.H. and Paul, D.R., *J. Polym. Sci., Part B: Polym. Phys. Ed.*, 1992, **30**, 817.
34. Weinkauff, D.H. and Paul, D.R., *J. Polym. Sci., Part B: Polym. Phys. Ed.*, 1992, **30**, 837.
35. Mizoguchi, M., Kamiya, Y. and Hirose, T., *J. Polym. Sci., Part B: Polym. Phys. Ed.*, 1991, **29**, 695.
36. Carfagna, C., Amendola, E., Giamberini, M., Mensitieri, G., Del Nobile, M.A. and Filippov, A.G., *Pol. Eng. Sci.*, 1995, **35** (2), 137–143.
37. Weinkauff, M., *Polym. Comm.*, 1988, **29**, 97.
38. Iannelli, P., Roviello, A. and Sirigu, A., *Eur. Pol. J.*, 1982, **18**, 759–762.
39. Roviello, A. and Sirigu, A., *Gazzetta Chimica Italiana*, 1987, **107**, 333–337.
40. Barton, J.M., *Advances in Polymer Science*, Vol. 72. Springer, Berlin, 1986.
41. Rozenberg, B.A., *Advances in Polymer Science*, Vol. 75. Springer, Berlin, 1986.
42. Smith, I.T., *Polymer*, 1961, **2**, 95.
43. Schecter, L., Wynstra, J. and Kurkji, R.P., *Ind. Eng. Chem.*, 1956, **48** (1), 94.
44. Barton, J.M., *Polymer*, 1980, **21**, 604.
45. Dobas, I., Eichler, J. and Klaban, J., *Collect. Czech. Chem. Commun.*, 1975, **40**, 2989.
46. Carfagna, C., Amendola, E. and Giamberini, M., *Macromol. Chem. Phys.*, 1994, **195**, 2307–2315.
47. Apicella, A., Nicolais, L., Carfagna, C., deNotaristefani, C. and Voto, C., *27th National SAMPE Symposium and Exhibition*, Vol. 27. SAMPE National Business Office, Azusa, CA, 1982.
48. Mika, T.F. and Bauer, R.S., in *Epoxy Resins, Chemistry and Technology*, ed. C.A. May. Marcel Dekker Inc., New York, 1988, p. 482.
49. Saunders, K.J., *Organic Polymer Chemistry*, 2nd ed. Chapman and Hall, London, 1988.
50. Finkelmann, H., *Adv. Polym. Sci.*, 1984, **60**, 99.
51. Barclay, G.G., Ober, C.K., Papathomas, K.I. and Wang, D.W., *J. Polym. Sci., Part A: Polym. Chem.*, 1992, **30**, 1831.
52. Barclay, G.G., McNamee, S.G., Ober, C.K., Papathomas, K.I. and Wang, D.W., *J. Polym. Sci., Part A: Polym. Chem.*, 1992, **30**, 1845.
53. Clough, S.B., Blumstein, A. and Hsu, E.C., *Macromolecules*, 1976, **9**, 123.
54. Barclay, G.G., Ober, C.K. and Papathomas, K.I., *Macromolecules*, 1992, **25**, 2947.
55. Roviello, A. and Sirigu, A., *Makromol. Chem.*, 1982, **183**, 895–904.
56. Finkelmann, Ringsdorf, H. and Wendorff, J.H., *Makromol. Chem.*, 1978, **179**, 273.
57. Marcelja, S., *J. Chem. Phys.*, 1974, **60**, 3599.
58. Pink, D.A., *J. Chem. Phys.*, 1975, **63**, 2533.
59. Carfagna, C., Roviello, A., Santagata, S. and Sirigu, A., *Makromol. Chem.*, 1986, **187**, 2123–2129.
60. Finkelmann, H., Schätzle, J., Kaufhold, W. and Pohl, L., *Freiburger Arbeitstagung Flüssigkristalle*, 15–17 März, Freiburg im Breisgau, 1989.
61. Landau, L., *Phys. Z. Sowjetunion*, 1937, **11**, 26.
62. de Gennes, P.G., *Mol. Cryst.*, 1971, **12**, 193.

63. de Gennes, P.G., *The Physics of Liquid Crystals*. Clarendon Press, Oxford, 1974.
64. de Gennes, P.G., in *Polymer Liquid Crystals*, ed. A. Ciferri, W.R. Krigbaum, R.B. Meyer, VCH, New York, 1991.
65. Giamberini, M., Amendola, E. and Carfagna, C., *Makromol. Chem. Rapid Commun.*, 1995, **16**, 97–105.
66. Canessa, G., Reck, B., Reckert, G. and Zentel, R., *Makromol. Chem., Macromol. Symp.*, 1986, **4**, 91.
67. de Vries, A., *J. Chem. Phys.*, 1972, **56** (9), 4489–4495.
68. Mitchell, G.R. and Windle, A.H., *Polymer*, 1983, **24**, 1513–1520.
69. Kaufhold, W., Finkelmann, H. and Brand, H.R., *Makromol. Chem.*, 1991, **192**, 2555–2579.
70. Ballauf, M., *Angew. Chem. Int. Engl. Adv. Mater.*, 1989, **28**, 1130.
71. Aharoni, S.M., *Macromolecules*, 1991, **24**, 295.
72. Barclay, G.G. and Ober, C.K., *Prog. Polym. Sci.*, 1993, **18**, 899.
73. Jones, R.E. Jr., Earl, J.D. and Hefner R.E. Jr., U.S. Patent No. 5, 248, 360.
74. Bhama, S. and Stupp, S., *Poly. Eng. Sci.*, 1990, **30** (10), 603.
75. Jakeman, E. and Raynes, E.P., *Phys. Lett.*, 1972, **A30**, 69.
76. Schadt, M. and Muller, F., *Inst. Elect. Electron. Engrs., Trans. Electron. Devices*, 1978, **25**, 1125.
77. Clark, M.G., *Mol. Cryst. Liq. Cryst.*, 1985, **127**, 1.
78. Janning, J.L., *Appl. Phys. Lett.*, 1972, **21**, 173.
79. Berreman, D., *Phys. Rev. Lett.*, 1972, **28**, 1683.
80. Meyerhofer, K., *Appl. Phys. Lett.*, 1976, **29**, 691.
81. Rowell, D.K., Raynes, E.P. and Shonks, I.A., *Mol. Cryst. Liq. Cryst.*, 1976, **34**, 105.
82. Kutty, T.R.N. and Fisher, A.G., *Mol. Cryst. Liq. Cryst.*, 1983, **99**, 310.
83. Matsuura, N., Mada, H., Aoyama, H., Yamazaki, Y. and Kobayashi, S., *Mol. Cryst. Liq. Cryst.*, 1981, **72**, 127.
84. Cognard, J., *Mol. Cryst. Liq. Cryst.*, 1982, **1**, 1.
85. Myrvold, B.O., *Liq. Cryst.*, 1988, **3**, 1255.
86. Costellano, J.A., *Mol. Cryst. Liq. Cryst.*, 1987, **94**, 12337.
87. Seo, D.S., Oh-Ide, T., Matsuda, H., Isogami, T.R., Muroi, K.I., Yabe, Y. and Kobayashi, S., *Mol. Cryst. Liq. Cryst.*, 1993, **231**, 95.
88. Toney, M.F., Russell, T.P., Logan, J.A., Kikuchi, H., Sands, J.M. and Kumar, S.K., *Nature*, 1995, **374**, 709.
89. Zhu, Y.M., *Mol. Cryst. Liq. Cryst.*, 1993, **231**, 95.
90. Saunders, K.J., *Organic Polymer Chemistry*. Chapman and Hall, New York, 1988.
91. Berreman, D.W., *Mol. Cryst. Liq. Cryst.*, 1973, **23**, 215.
92. Doane, J.W., Vaz, N.A.P., Wu, B.G. and Zumer, S., *Appl. Phys. Lett.*, 1986, **48**, 269.
93. Doane, J.W., Chidichimo, G. and Vaz, N.A.P., U.S. Patent No. 4,688,900, 1987.
94. Vaz, N.A. and Montgomery, G.P. Jr., *Mol. Cryst. Liq. Cryst.*, 1987, **146**, 1.
95. Wu, B.G., West, J.L. and Doane, J.W., *J. Appl. Phys.*, 1987, **62**, 3925.
96. Vaz, N.A. and Montgomery, G.P. Jr., *J. Appl. Phys.*, 1987, **62**, 3161.
97. *UV and EB Curing Formulation for Printing Inks, Coating and Paints*. SITA Technology, London, 1988.
98. Yamagishi, F.G., Miller, L.J. and van Ast, C.I., *Proc. SPIE*, 1989, **1080**, 24.
99. Boutevin, B., *Appl. Polym. Sci. Part A: Polym. Chem.*, 1993, **50**, 2065–2073.
100. Chien, L.C., Lin, C., Fredley, D.S. and McCargar, J.W., *Macromolecules*, 1992, **25**, 133–137.
101. Chien, L.C., Cada, L.G. and Xie, L., *Liq. Cryst.*, 1992, **12** (5), 853–861.
102. Carfagna, C., Amendola, E., Giamberini, M., Filippov, A.G. and Bauer, R.S., *Liq. Cryst.*, 1993, **19**, 571–584.
103. J.L. West, *Liquid Crystalline Polymers*, ACS Symposium Series, **435**, 491, annual.